Chapter 12

Tool of the Complete Optimal Control for Variable Speed Electrical Drives

Marian Gaiceanu

Additional information is available at the end of the chapter

http://dx.doi.org/10.5772/57521

1. Introduction

The main objective of the chapter is to use Matlab software in order to develop the optimal control knowledge in relation to the biggest worldwide power consumers: electrical machines. These two major components, optimal control and electrical machines form an optimal drive system. The proposed drive system conducts to the energy efficiency increasing during transient regimes (starting, stopping and reversing), therefore reducing the impact upon the environment. Taking into account the world energy policies, the chapter is strategically oriented towards the compatibility with the priority requirements from world research programmes. This chapter will offer an original Matlab tool in order to implement a highly performant control for electrical drives. The optimal solution provided by the optimal problem is obtained by numerical integration of the matrix Riccati differential equation (MRDE). The proposed optimal control, based on energetic criterion, can be implemented on-line by using a real time experimental platform. The solution has three terms: the first term includes the reference state of the electrical drive system, the second term assures a fast compensation of the disturbance (i.e. the load torque in case of the electrical drives) by using feedforward control, and the third is the state feedback component. Therefore, there is a completed optimal control for linear dynamic systems. The simulation and experimental results will be provided. By using knowledge regarding the electrical machines, electrical and mechanical measurements, control theory, digital control, and real time implementation, a high degree of interdisciplinarity is obtained in the developed Matlab tool The optimal problem statement is without constraints; by choosing adequate weighting matrices, the magnitude constraints of control and of state variable are solved.

Matlab is a widespread software used both in academia and research centres. The author of this chapter facilitates the easy understanding and implementation of the highly efficient electrical drive systems by using Matlab software. The energy problem is one of the most important aspects related to the sustainable growth of the industrial nations. On the one hand, the industrial systems and the increased quality of life require every year a higher quantity of electrical energy produced; on the other hand, the same quality of life requires the generation and the harnessing of this energy with low pollution.

On the one hand, the electrical machines are the main worldwide energy consumer (Siemens), (Tamimi, *et al*., 2006). Therefore, the focus of the research on this system type is essential in order to minimize the energetical losses. A seemingly insignificant reduction of electricity consumed by each electrical motor has particularly important consequences at national/ international level, primarily by reducing consumption of fossil fuels widely used to generate electricity, therefore contributing also to CO2 emissions reduction. Researches in this area are at different levels: I) direct conversion by redesigning the electric motors to obtain high efficiency; II) the power electronic systems by introducing static converters with diminished switching losses; III) control implementation of the conversion process by using the enhanced capabilities of new generation digital signal processor DSP (Veerachary M., 2002).

The efficiency of the motor is high on steady state operation, but very low in transients. On the other hand, the associated equipment for energy conversion purposes, i.e. power converters together with the control subsystem, assures both high static and dynamic performances (related to the settling time, error minimizing and so on), but they are not related to energy expenditure. The analysis of various technical publications shows a yearly increase of energy expenditure of the electrical motors, with a rate of 1,5% in Europe, 2,2% in USA, 3,1% in Japan; these values can even reach the rate of 13%, depending on the development of calculus technology (Matinfar, *et al.,* 2005), (Gattami, *et al.,*2005), (COM, 2006).

Dynamic programming tool is very useful to obtain the optimal solution, but the values of the torque and speed must be known in advance (Mendes, *et al*., 1996). In machine building industry the operating cycle is well-known (Lorenz, *et al*., 1992; 1998) therefore, the dynamic programming is an efficient tool only for these type of applications. But the optimization method fails when the conventional electrical drives are taken into account because the load torque could not be known in advance, i.e. at the final time of the process.

The optimal solution (Gaiceanu, 1997) provided in this chapter overcomes this type of scientific barrier (Rosu, 1985), making possible implementation of the optimal solution to any type of application, without knowing the speed and load torque in advance. As it is nonrecursive, determined on the basis of variational methods (by integrating the Matrix Riccati Differential Equation), the optimal solution can be calculated on-line without memorizing it from the final time to the initial time, as in the recursive method. Therefore, the nonrecursive solution can be implemented to any type of electrical motor with any load variation, for any operating dynamical regimes.

On the other hand, the problem of increasing power conversion efficiency in the drive systems is the subject of numerous worldwide studies. The Siemens Automation (Siemens) claims the

http://dx.doi.org/10.5772/57521

optimization based on the speed controller which can be optimized in the time or in the frequency range. In the time range, the symmetrical optimum method can be used. In the frequency range, the optimizing is done according to the amplitude and phase margin rules, known from the control theory, but these are the conventional controls that are used in drives.

The interdisciplinarity of the chapter consists of using specific knowledge from the fields of: energy conversion, power converters, Matlab/Simulink simulation software, real time implementation based on dSPACE platform, electrotechnics, and advanced control techniques.

This chapter is focused on mathematical modelling, optimal control development on power inverter, Matlab implementation and analysis of the optimal control solution in order to minimize the electric input energy of the drive system. The Matlab on-line solution can be downloaded in real-time platforms, as dSPACE or dsPIC Digital Signal Controllers (Gaiceanu, *et al.*, 2008).

The practical implication of using the proposed method is the on-line calculation of the optimal control solution. The main lines of the research methodology are:

- The optimal control of the dynamical electrical drives problem formulation;
- The optimal control solution;
- The numerical simulation results;
- The implementation of the optimal control.

The strategy of the optimal control electrical drive system is to use both the conventional control during the steady state and the developed optimal control during the transients. The conventional control is based on the rotor field orientated control using Proportional Integral controllers. If the speed error is different from zero, the software switch will enable the optimal control, else will enable the conventional control. Both types of control are developed in the next Sections.

2. Mathematical model of the variable speed electrical drives (VSED)

There are variable speed DC and AC drives. A DC drive system controlled by armature voltage at constant field is a linear, invariant and controllable dynamic system. Variable speed AC drives are mostly used in connection with induction and synchronous electrical machines. The modern drives contain the energy source, the power converters, the electrical machines, the mechanical power transmission and the load, linked by an adequate control. The well-known mathematical model of the vector controlled AC drive using three phase squirrel cage induction machine in rotor field coordinates supplied from the current inverter, operating at the constant flux (Leonhard, 1996) becomes a linear system (Gaiceanu, 2002). For the electrical drives having the power less than 50 kW, the power loss of the converter could be neglected. In order to compute the optimal solution for synchronous Drive system, the control in rotor

field oriented reference frame of surface mounted permanent magnet synchronous motor (PMSM) drives is used. The control loops (torque and flux) are performed in rotor field reference frame. By setting a zero value of direct current stator component, the mathematical model of the PMSM becomes linear. Therefore, there is a common mathematical model of the electrical drives, described by the linear state space standard form representation:

$$\dot{x}(t) = A\dot{x}(t) + B\dot{u}(t) + G\dot{w}(t) \quad (1)$$

where $\boldsymbol{x}(t)$ is the state vector, $\mathbf{u}(t)$ is the control vector, and the perturbation vector is the load torque $w(t)=[T_L\ (t)]$.

Taking into consideration the most used electrical machine, the three-phase squirrel cage induction machine, the electrical drive based on it will be explained as follows. Starting from the nameplate data of the induction machine (Fig.1), the main parameters of the electrical motor can be found (Appendix 1).

```
%Nominal Power (mechanical power)
Pn=750;% kW
%Stator resistance
Rs=1.7;       %[ohmi]
%rotor resistance
Rr=2.55;      %[ohmi]
%stator leakage inductance
Lss=0.00986;  %[H]
%rotor leakage inductance
Lrs=0.01002;  %[H]
%mutual inductance
Lm=0.2680; %[H]
%total equivalent inertia mass
J=0.002;      %[kgm^2]
% number of pole pairs
p=2;
%power factor
cosfi=0.71;
%rated efficiency
etan=0.794;
%rated speed
nn=1480;
%frequency
f1=50;        %[Hz]
```

Figure 1. Nameplate data of the electrical machine (three phase induction motor)

The mathematical model of the three phase squirrel cage induction machine (IM) in rotor field reference system operating at constant flux is (Leonhard, 1996):

http://dx.doi.org/10.5772/57521

$$\begin{cases} \dfrac{\mathrm{d}q}{\mathrm{d}t} = \dfrac{\omega_{\mathrm{e}}}{p} + \dfrac{i_{qs}}{T_r i_{mr}} \\ \dfrac{J}{p}\dfrac{\mathrm{d}\omega_{\mathrm{e}}}{\mathrm{d}t} = T_{\mathrm{e}} - \dfrac{F}{p}\omega_{\mathrm{e}} - T_L \\ T_{\mathrm{e}} = k_m \cdot i_{mr} \cdot i_{qs}, \end{cases} \quad \text{(a)}$$

$$\begin{cases} T_r \dfrac{\mathrm{d}i_{mr}}{\mathrm{d}t} + i_{mr} = i_{ds} \\ \dfrac{\mathrm{d}q}{\mathrm{d}t} = \dfrac{\omega_{\mathrm{e}}}{p} + \dfrac{i_{qs}}{T_r i_{mr}} \\ \dfrac{J}{p}\dfrac{\mathrm{d}\omega_{\mathrm{e}}}{\mathrm{d}t} = T_{\mathrm{e}} - \dfrac{F}{p}\omega_{\mathrm{e}} - T_L \\ T_{\mathrm{e}} = k_m \cdot i_{mr} \cdot i_{qs}, \end{cases} \quad \text{(a)}$$

i_{mr} – rotor magnetizing current; i_{ds}, i_{qs} – f lux and torque components o

T_e – electromagnetic torque, TL – load torque, p – number of pole pair

Ts, Tr stator and rotor time constants;

q – angle of the magnetizing current vector; w_e, w – electrical and mec

where i_{mr} – rotor magnetizing current; i_{ds}, i_{qs} – f lux and torque components of the stator current;

T_e – electromagnetic torque, TL – load torque, p – number of pole pairs, F – viscous force; (2)

Ts, Tr stator and rotor time constants;

q – angle of the magnetizing current vector; w_e, w – electrical and mechanical rotor speed,

$$\omega_{\mathrm{e}} = p\omega \quad \text{(b)}$$

with L_m – magnetizing inductance, s_r – rotor magnetizing dispersion f

with L_m – magnetizing inductance, σ_r – rotor magnetizing dispersion factor.

$$K_m = \frac{2}{3} p \cdot \frac{L_m}{1+\sigma_r} \quad \text{(c)}$$

$$K_m = \frac{2}{3} p \cdot \frac{L_m}{1+\sigma_r} \quad \text{(c)}$$

(1)

By varying the flux component of the stator current, i_{ds}, the magnet

By varying the flux component of the stator current, i_{ds}, the magnetizing current response, $i_{mr}(t)$, can have significant delay. By using an adequate control of pow

By varying the flux component of the stator current, i_{ds}, the magnetizing current response, $i_{mr}(t)$, can have significant delay. By using an adequate control (Guiatni, 2002), the rotor magnetizing current, i_{mr}, can be maintained at th

By varying the flux component of the stator current, i_{ds}, the magnetizing current response, $i_{mr}(t)$, can have significant delay. By using an adequate control of power inverter (Guiatni, 2002), the rotor magnetizing current, i_{mr}, can be maintained at the constant value, and according to the mathematical model of the IM (1a), the flux component of the stator current, i_{ds}, equates the rotor magnetizing current): $i_{mr}=i_{ds}$=ct.. Therefore, the standard state space form of the IM mathematical model can be obtained (Fig.2):

By varying the flux component of the stator current, i_{ds}, the magnetizing current response, $i_{mr}(t)$, can have significant delay. By using an adequate control of power inverter (Guiatni, 2002), the rotor magnetizing current, i_{mr}, can be maintained at th

By varying the flux component of the stator current, i_{ds}, the magnetizing current response, $i_{mr}(t)$, can have significant delay. By using an adequate control of power inverter (Guiatni, 2002), the rotor magnetizing current, i_{mr}, can be maintained at the constant value, and according to the mathematical model of the IM (1a), the flux component of the stator current, i_{ds}, equates the rotor magnetizing current): $i_{mr}=i_{ds}$=ct.. Therefore, the standard state space form of the IM mathematical model can be obtained (Fig.2):

By varying the flux component of the stator current, i_{ds}, the magnetizing current response, $i_{mr}(t)$, can have significant delay. By using an adequate control of power inverter (Guiatni, 2002), the rotor magnetizing current, i_{mr}, can be maintained at th

By varying the flux component of the stator current, i_{ds}, the magnetizing current response, $i_{mr}(t)$, can have significant delay. By using an adequate control of power inverter (Guiatni, 2002), the rotor magnetizing current, i_{mr}, can be maintained at the constant value, and according to the mathematical model of the IM (1a), the flux component of the stator current, i_{ds}, equates the rotor magnetizing current): $i_{mr}=i_{ds}$=ct.. Therefore, the standard state space form of the IM mathematical model can be obtained (Fig.2):

```
%   INITIAL DATA
     isd=Idref;
     imr=isd;
     km=2*Lm*imr/(3*(1+sigmar));
     Fv=0.0006;
%   The matrix of the system
    A=[-Fv/J      0;
         1        0];
%   The control vector
     kq=1/(Tr*imr);
     B=[   km/J;
           kq ];
%   The perturbation vector
    G=[-1/J;
        0  ];
%   The output matrix
    Ct=[1  0];
%   D=[0  0];
```

Figure 2. Standard space state form characterization of the three phase Induct

Figure 2. Standard space state form characterization of the three phase Induction Motor

3. Optimal control problem statement

The common objectives of the optimal control drive systems are: the smooth dynamic response, without oscillations; achieving the desired steady state; the fast compensation of the load torque; energy minimization. Taking into consideration the main objectives of the electrical drive system, the following Section describes the chosen quadratic performance criterion.

3.1. The quadratic performance criterion

The functional cost or the quadratic performance criterion is chosen such that the electrical input power, the energy expended in the stator windings of the electrical machines is minimized, and the cost of the control is weighted. Therefore, the performance functional quadratic criterion (Rosu, 1985), (Gaiceanu, 2002), (Athans, 2006), is as follows:

$$J=\frac{1}{2}\left[\boldsymbol{x}(t_1)-\boldsymbol{x}_1\right]^T \boldsymbol{S}\left[\boldsymbol{x}(t_1)-\boldsymbol{x}_1\right]+\frac{1}{2}\int_{t_0}^{t_1}\left[\boldsymbol{x}^T(t)\,\boldsymbol{Q}\boldsymbol{x}(t)+\boldsymbol{u}^T(t)\,\boldsymbol{R}\boldsymbol{u}(t)\right]dt \tag{3}$$

in which, taking into consideration a starting of the IM, the initial conditions consists of the initial time t_0=0[s] and the initial state vector $\boldsymbol{x}(t_0)=[\omega(t_0)\quad q(t_0)]^T=[0\quad 0]^T$, T-being the transpose symbol of the initial state vector. The final condition is the required final state, $\mathbf{x}_1$. The components of the $\mathbf{x}_1$ are: the desired angular velocity, ω^*_{m}, and a free rotor magnetizing angle value, q^*=0, i.e $\boldsymbol{x}_1=\begin{bmatrix}\omega_m^*\\ 0\end{bmatrix}$; the final time, t_1=0.9[s]. The value of the final time is established by the feasibility condition, i.e. the value of it is taken from the obtained final time of the starting process with conventional control (Proportional Integral controllers). In order to exist and to obtain a unique optimal solution, the weighting matrices must be chosen according to: $\mathbf{S}\geq 0$, $\mathbf{R}>0$, $\mathbf{Q}\geq 0$. The weighted matrix **S** minimizes the square error between the reached state $\boldsymbol{x}(t_1)$, and the desired state, $\mathbf{x}_1$, in the fixed time t_1, the weighted matrix **R** minimizes the control effort, $\boldsymbol{u}(t)=i_{qs}(t)$, and the weighted matrix **Q** minimizes the expended energy in the motor windings. The optimal control problem taken into account in this chapter is with free-end point, fixed time and unconstrained. The restrictions of the magnitude for the control vector, and state vectors are managed through the design process, by an adequate choice of the weighting matrices.

3.2. The solution of the optimal control problem.

The existence and the unicity of the optimal control problem solution are based on the controllability and observability of the system (1). The system (1) being controllable and completely observable, the weighting matrices are chosen such that **Q, S ≥ 0** are positive semidefinite, and matrix **R>0** is positive definite (Gaiceanu, 2002). In this way, the existence and the unicity of the optimal control problem solution are assured.

By using variational method, the Hamiltonian of the optimal control problem is given by

http://dx.doi.org/10.5772/57521

$$H(p,x,u,t)=\frac{1}{2}\left[\boldsymbol{x}^T(t)\,\boldsymbol{Q}\boldsymbol{x}(t)+\boldsymbol{u}^T(t)\boldsymbol{R}\boldsymbol{u}(t)+\boldsymbol{y}^T(t)\cdot\left(\boldsymbol{A}\boldsymbol{x}(t)+\boldsymbol{B}\boldsymbol{u}(t)+\boldsymbol{G}\boldsymbol{w}(t)\right)\right] \tag{4}$$

in which $\boldsymbol{y}(t)\in\Re^2$ is the costate vector.

The condition **R>0** assures the inversability of the eigenvectors and that the optimal solution has a minimum (Gaiceanu, 2002). The optimal control minimizing the Hamiltonian (4) is given by

$$u^*(t)=-\boldsymbol{R}^{-1}\boldsymbol{B}^T\boldsymbol{y}(t) \tag{5}$$

By using the canonical system, the solutions of the costate $\boldsymbol{y}(t)$ and state vectors $\boldsymbol{x}(t)$ can be obtained:

$$\begin{bmatrix}\dot{\boldsymbol{x}}(t)\\ \dot{\boldsymbol{y}}(t)\end{bmatrix}=\begin{bmatrix}\boldsymbol{A} & -\boldsymbol{B}\boldsymbol{R}^{-1}\boldsymbol{B}^T\\ -\boldsymbol{Q} & -\boldsymbol{A}^T\end{bmatrix}\begin{bmatrix}\boldsymbol{x}(t)\\ \boldsymbol{y}(t)\end{bmatrix}+\begin{bmatrix}\boldsymbol{G}\\ \boldsymbol{0}\end{bmatrix}\boldsymbol{w}(t) \tag{6}$$

The boundary conditions of the canonical system (5) are:

-the initial state $\boldsymbol{x}(0)=\boldsymbol{x}_o$;

-the transversality condition of the costate vector:

$$\boldsymbol{y}(t_1)=\left.\frac{\partial\boldsymbol{\lambda}(t)}{\partial\boldsymbol{x}}\right|_{t=t_1}=\boldsymbol{S}\left[\boldsymbol{x}(t_1)-\boldsymbol{x}_1\right] \tag{7}$$

$$\boldsymbol{y}(t_1)=\boldsymbol{S}\left[\boldsymbol{x}(t_1)-\boldsymbol{x}_1\right]=100\begin{bmatrix}\omega(t_1)\\ q(t_1)\end{bmatrix}-\begin{bmatrix}15707{,}96\\ 0\end{bmatrix},$$

where the weighting matrix $\boldsymbol{S}=\begin{bmatrix}100 & 0\\ 0 & 0\end{bmatrix}$, and q is the angle of the rotor magnetizing flux.

The integration of the canonical system leads to the well-known matrix Riccati differential equation and the associate vectorial equation (Rosu, 1985), (Gaiceanu, 2002), (Athans, *et al.*, 2006). The integration of these two equations is a very difficult task because the Riccati equation is nonlinear, its solution is recursive (which can be calculated backward in time) (Gattami, *et al.*, 2005), (Jianqiang, *et al.*, 2007), (Rosu, 1985). Moreover, the backward computation needs to know a priori the variation of the perturbation vector $\mathbf{w}(t)$ during the control interval $[0, t_1]$. In most electrical drives the last condition cannot be accomplished.

A nonrecursive solution of the Riccati equation has been developed by using two linear transformations (Rosu, *et al.*, 1998). *The first transformation* changes actual time t into t_1-t, that is time remaining until the end of the optimal process.

$$\tau = t_1 - t = 0.9 - t, \tag{8}$$

In order to use only the negative eigenvalues for the computation of the fundamental matrix of the system (1), *the second transformation* is made. Therefore, by defining new vectors $\mathbf{p}(\tau)$, $\mathbf{q}(\tau)$, $\mathbf{r}(\tau)$,

$$\begin{bmatrix} \overset{\circ}{\boldsymbol{p}}(\tau) \\ \overset{\circ}{\boldsymbol{q}}(\tau) \end{bmatrix} = \begin{bmatrix} -\boldsymbol{A} & \boldsymbol{B}\boldsymbol{R}^{-1}\boldsymbol{B}^T \\ \boldsymbol{Q} & \boldsymbol{A}^T \end{bmatrix} \begin{bmatrix} \boldsymbol{p}(\tau) \\ \boldsymbol{q}(\tau) \end{bmatrix} - \begin{bmatrix} \boldsymbol{G} \\ \boldsymbol{0} \end{bmatrix} \boldsymbol{r}(\tau) \tag{9}$$

and by noting the canonical matrix (4×4) of the system (1) as:

$$\begin{bmatrix} -\boldsymbol{A} & \boldsymbol{B}\boldsymbol{R}^{-1}\boldsymbol{B}^T \\ \boldsymbol{Q} & \boldsymbol{A}^T \end{bmatrix} = \boldsymbol{M} \tag{10}$$

the eigenvalues λ_i, $i = \overline{1,\ 4}$ of the canonical matrix $\mathbf{M}$ can be computed with:

$$\det\left[\lambda \boldsymbol{I} - \boldsymbol{M}\right] = 0 \tag{11}$$

By using the developed Matlab file from Appendix 3, the appropriate negative eigenvalues position placed on the main diagonal of the eigenvalues matrix, $\mathbf{D}$, with $\text{diag}(\boldsymbol{D}) = \{\lambda_1,\ \lambda_2,\ \lambda_3,\ \lambda_4\}$, can be obtained:

$$\begin{bmatrix} \lambda_1 & 0 & 0 & 0 \\ 0 & \lambda_2 & 0 & 0 \\ 0 & 0 & -\lambda_1 & 0 \\ 0 & 0 & 0 & -\lambda_2 \end{bmatrix} = \begin{bmatrix} 5.1663 & 0 & 0 & 0 \\ 0 & 0.7205 & 0 & 0 \\ 0 & 0 & -5.1663 & 0 \\ 0 & 0 & 0 & -0.7205 \end{bmatrix} = \begin{bmatrix} \Lambda & \boldsymbol{0} \\ \boldsymbol{0} & -\Lambda \end{bmatrix}, \tag{12}$$

in which

$$\Lambda = \begin{bmatrix} \lambda_1 & 0 \\ 0 & \lambda_2 \end{bmatrix} = \begin{bmatrix} 5.1663 & 0 \\ 0 & 0.7205 \end{bmatrix}. \tag{13}$$

http://dx.doi.org/10.5772/57521

In the Appendix 3 the proper position of the eigenvalues and the eigenvectors of the linear system (1) is provided. By using the program sequence from Appendix 3, the stability of the system is assured and the corresponding matrix of the eigenvectors is obtained:

$$W = \begin{bmatrix} 0.9877 & -0.5906 & -0.9740 & -0.5702 \\ -0.1567 & 0.8070 & -0.2268 & -0.8215 \\ 0.0004 & -0.0001 & 0.0004 & 0.0000 \\ -0.0000 & 0.0011 & 0.0000 & 0.0011 \end{bmatrix} \tag{14}$$

By knowing the inverse of the eigenvector matrix $\mathbf{W}^{-1}$

$$W-1 \ = 1.0e+003 \ * \begin{bmatrix} 0.0005 & 0.0001 & 1.3542 & 0.3153 \\ 0.0000 & 0.0006 & 0.3158 & 0.4549 \\ -0.0005 & 0.0000 & 1.3732 & -0.2178 \\ 0.0000 & -0.0006 & -0.3271 & 0.4469 \end{bmatrix} \tag{15}$$

the new vectors, $\mathbf{m}(\tau)$, $\mathbf{n}(\tau)$, $\mathbf{p}(\tau)$, $\mathbf{q}(\tau)$ are introduced as follows:

$$\begin{bmatrix} m(\tau) \\ n(\tau) \end{bmatrix} = W^{-1} \begin{bmatrix} p(\tau) \\ q(\tau) \end{bmatrix}, \tag{16}$$

$$\begin{bmatrix} p(\tau) \\ q(\tau) \end{bmatrix} = W \begin{bmatrix} m(\tau) \\ n(\tau) \end{bmatrix} \tag{17}$$

By introducing (15) and (16) transformations in (8), the following differential system is obtained:

$$W \begin{bmatrix} \overset{\circ}{m}(\tau) \\ \overset{\circ}{n}(\tau) \end{bmatrix} = M \, W \begin{bmatrix} m(\tau) \\ n(\tau) \end{bmatrix} - \begin{bmatrix} G \\ 0 \end{bmatrix} r(\tau) \tag{18}$$

Therefore, the canonical system can be written in terms of $\mathbf{n}(\tau)$, and $\mathbf{m}(\tau)$ vectors:

$$\begin{bmatrix} \overset{\circ}{m}(\tau) \\ \overset{\circ}{n}(\tau) \end{bmatrix} = W^{-1} M W \begin{bmatrix} m(\tau) \\ n(\tau) \end{bmatrix} - W^{-1} \begin{bmatrix} G \\ 0 \end{bmatrix} r(\tau) \tag{19}$$

By using the well-known relation

$$\boldsymbol{W}^{-1}\boldsymbol{M}\boldsymbol{W}=\begin{bmatrix}\Lambda & 0\\ 0 & -\Lambda\end{bmatrix} \tag{20}$$

and by noting the new vector **H** as:

$$\boldsymbol{W}^{-1}\begin{bmatrix}\boldsymbol{G}\\ \boldsymbol{0}\end{bmatrix}=\boldsymbol{H}=\begin{bmatrix}-52.6495\\ -0.2471\\ -47.8790\\ 23.0137\end{bmatrix}, \tag{21}$$

the new form of the canonical system can be obtained:

$$\begin{bmatrix}\overset{\circ}{\boldsymbol{m}}(\tau)\\ \overset{\circ}{\boldsymbol{n}}(\tau)\end{bmatrix}=\begin{bmatrix}\Lambda & 0\\ 0 & -\Lambda\end{bmatrix}\begin{bmatrix}\boldsymbol{m}(\tau)\\ \boldsymbol{n}(\tau)\end{bmatrix}-\boldsymbol{H}\cdot\boldsymbol{r}(\tau) \tag{22}$$

The solution of the new canonical system (21) can be obtained by using the following equation:

$$\begin{bmatrix}\boldsymbol{m}(\tau)\\ \boldsymbol{n}(\tau)\end{bmatrix}=\begin{bmatrix}\boldsymbol{e}^{\Lambda\tau} & 0\\ 0 & \boldsymbol{e}^{-\Lambda\tau}\end{bmatrix}\begin{bmatrix}\boldsymbol{m}(0)\\ \boldsymbol{n}(0)\end{bmatrix}-\int_0^{\tau}\begin{bmatrix}\boldsymbol{e}^{\Lambda\beta} & 0\\ 0 & \boldsymbol{e}^{-\Lambda\beta}\end{bmatrix}\boldsymbol{H}\boldsymbol{r}(\beta)\mathrm{d}\beta \tag{23}$$

As it can be observed the solution of the canonical system (22) solution contains both the positive, $\boldsymbol{e}^{\Lambda\tau}$, and the negative exponentials, $\boldsymbol{e}^{-\Lambda\tau}$. It is well-known that the positive exponentials produce the instability of the solution. Moreover, in order to obtain the analytical solution of the system (22) the load torque ($r(\tau)$ or $\mathbf{w}(t)$) at the final time, t_1, must be known in advance. For the most used electrical drive system this condition is hardly accomplished because the load torque cannot be known in advance, at the final time.

A numerical solution of the optimal problem is proposed. The advantage of maintaining the sampled signal at the same value during the sampled period is that the zero order hold (ZOH) offers a brilliant solution to know the load torque at the final time. Therefore, under this assumption, the solution **(22)** is computed each sampled time, T, and the perturbation vector **r** has constant value during it:

$$\begin{bmatrix}\boldsymbol{m}(\tau)\\ \boldsymbol{n}(\tau)\end{bmatrix}=\begin{bmatrix}\boldsymbol{e}^{\Lambda\tau} & 0\\ 0 & \boldsymbol{e}^{-\Lambda\tau}\end{bmatrix}\begin{bmatrix}\boldsymbol{m}(0)\\ \boldsymbol{n}(0)\end{bmatrix}+\begin{bmatrix}\boldsymbol{I}-\boldsymbol{e}^{\Lambda\tau} & 0\\ 0 & \boldsymbol{I}-\boldsymbol{e}^{-\Lambda\tau}\end{bmatrix}\begin{bmatrix}\boldsymbol{H}_1\\ \boldsymbol{H}_2\end{bmatrix}r \tag{24}$$

http://dx.doi.org/10.5772/57521

where **I** is the identity matrix.

The obtained solution of the canonical system (23) is:

$$\begin{bmatrix} m_1(\tau) \\ m_2(\tau) \\ n_1(\tau) \\ n_2(\tau) \end{bmatrix} = \begin{bmatrix} e^{(5.1663)\cdot\tau} & 0 & 0 & 0 \\ 0 & e^{(0.7205)\cdot\tau} & 0 & 0 \\ 0 & 0 & e^{-(5.1663)\cdot\tau} & 0 \\ 0 & 0 & 0 & e^{-(0.7205)\cdot\tau} \end{bmatrix} \cdot \begin{bmatrix} m_1(0) \\ m_2(0) \\ n_1(0) \\ n_2(0) \end{bmatrix} + \begin{bmatrix} 1-e^{(5.1663)\cdot\tau} & 0 & 0 & 0 \\ 0 & 1-e^{(0.7205)\cdot\tau} & 0 & 0 \\ 0 & 0 & 1-e^{-(5.1663)\tau} & 0 \\ 0 & 0 & 0 & 1-e^{-(0.7205)\cdot\tau} \end{bmatrix} \cdot \begin{bmatrix} -52.6495 \\ -0.2471 \\ -47.8790 \\ 23.0137 \end{bmatrix} \cdot r. \tag{25}$$

The negative exponentials can be obtained by extracting **m**(0) function on the **m**(τ). In this way, the first equation of the system **(24)** becomes:

$$\begin{bmatrix} \boldsymbol{m}(0) \\ \boldsymbol{n}(\tau) \end{bmatrix} = \begin{bmatrix} \boldsymbol{e}^{-\Lambda\cdot\tau} & 0 \\ 0 & \boldsymbol{e}^{-\Lambda\cdot\tau} \end{bmatrix} \cdot \begin{bmatrix} \boldsymbol{m}(\tau) \\ \boldsymbol{n}(0) \end{bmatrix} + \begin{bmatrix} \boldsymbol{I}_2 - \boldsymbol{e}^{-\Lambda\cdot\tau} & 0 \\ 0 & \boldsymbol{I}_2 - \boldsymbol{e}^{-\Lambda\cdot\tau} \end{bmatrix} \cdot \begin{bmatrix} \boldsymbol{H}_1 \\ \boldsymbol{H}_2 \end{bmatrix} \cdot r \tag{26}$$

where

$$\boldsymbol{I}_2 = \begin{bmatrix} 1 & 0 \\ 0 & 1 \end{bmatrix} \tag{27}$$

The negative exponentials of the system **(25)** guarantee the stability of the system (1).

The transversality condition (6), in terms of **m** and **n** vectors, is as follows:

$$\boldsymbol{n}(0) = \boldsymbol{E} \cdot \boldsymbol{m}(0) + \boldsymbol{F} \cdot \boldsymbol{x}_f \tag{28}$$

where,

$$\boldsymbol{E} = \left[\boldsymbol{S}\boldsymbol{W}_{12} - \boldsymbol{W}_{22}\right]^{-1}\left[\boldsymbol{W}_{21} - \boldsymbol{S}\boldsymbol{W}_{11}\right] = \begin{bmatrix} 1.0215 & -0.0320 \\ -0.0127 & -0.9811 \end{bmatrix} \tag{29}$$

$$F = \left[SW_{12} - W_{22} \right]^{-1} S = \begin{bmatrix} -1.0504 & 0 \\ 0.0404 & 0 \end{bmatrix} \tag{30}$$

By expressing $\mathbf{n}(\tau)$ function on $\mathbf{m}(\tau)$, the following equation can be deducted :

$$n(\tau) = Z(\tau) \cdot m(\tau) + e^{-\Lambda \cdot \tau} \cdot E \cdot \left(I_2 - e^{-\Lambda \cdot \tau} \right) \cdot H_1 \cdot r + e^{-\Lambda \cdot \tau} \cdot F \cdot x_1 + \left(I_2 - e^{-\Lambda \cdot \tau} \right) \cdot H_2 \cdot r \tag{31}$$

where

$$Z(\tau) = e^{-\Lambda \cdot \tau} \cdot E \cdot e^{-\Lambda \cdot \tau} \tag{32}$$

Going back through the reverse transformations from $\mathbf{m}(\tau)$, $\mathbf{n}(\tau)$ vectors to $\mathbf{p}(\tau)$, $\mathbf{q}(\tau)$ vectors, from the used τ time to the current time t, the state $\mathbf{x}(t)$ and costate $\mathbf{y}(t)$ expressions can be obtained. The costate vector at current time is as follows:

$$y(t) = P(t_1 - t) \cdot x(t) - K_1(t_1 - t) \cdot x_1 - K_2(t_1 - t) \cdot w \tag{33}$$

where the matrix $\mathbf{P}(t_1-t)$ is the solution of the matrix Riccati diferential equation, and the matrices$\mathbf{K}_1(t_1-t)$ and $\mathbf{K}_2(t_1-t)$ vector have the form:

$$K_1(t_1 - t) = -v(t_1 - t) \cdot e^{-\Lambda \cdot (t_1 - t)} \cdot F, \tag{34}$$

$$K_2(t_1 - t) = -v(t_1 - t) \cdot \left[e^{-\Lambda \cdot (t_1 - t)} \cdot E \cdot \left(I - e^{-\Lambda \cdot (t_1 - t)} \right) \cdot H_1 + \left(I - e^{-\Lambda \cdot (t_1 - t)} \right) \cdot H_2 \right], \tag{35}$$

The $\mathbf{v}$ matrix is as follows:

$$v(\tau) = \left[W_{22} - P(\tau) W_{12} \right]. \tag{36}$$

The solution of the optimal control problem has three components (Fig.3):

1. the state feedback $R^{-1} \cdot B^T P(t_1 - t) \cdot x(t)$, in order to assure the stability of the system;
2. the compensating feedforward load torque $R^{-1} \cdot B^T K_2(t_1 - t) \cdot w$, for fast compensation of the main perturbation, i.e. the load torque;
3. the reference component $R^{-1} \cdot B^T K_1(t_1 - t) \cdot x_1$, to track accurately the reference signal.

http://dx.doi.org/10.5772/57521

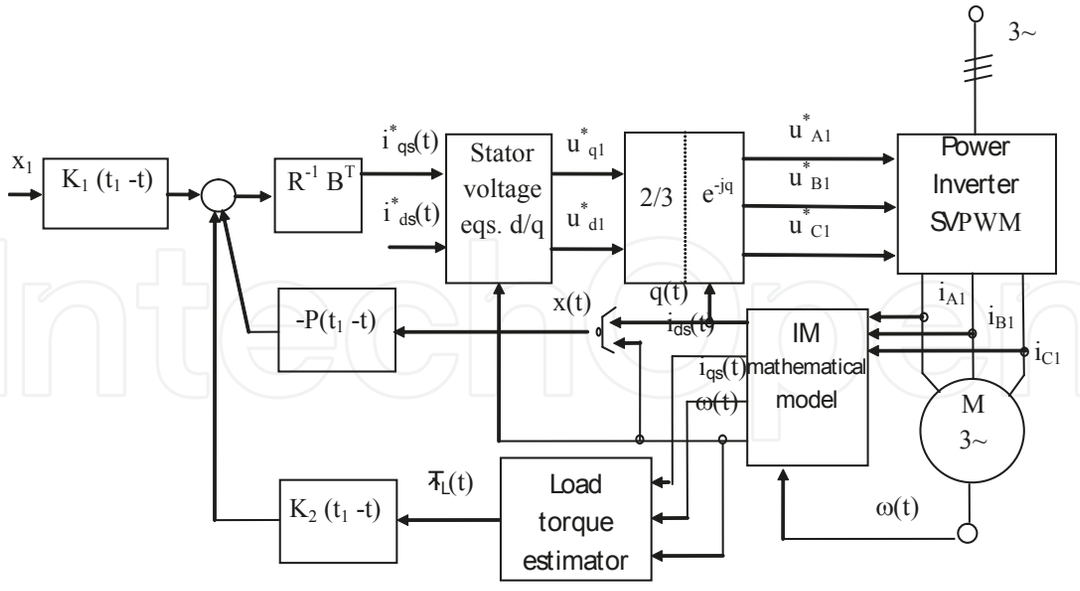

Figure 3. Optimal control (i^*_{sq}) implementation into three phase IM Drive System supplied by the Voltage Power Source Inverter

The optimal control, at any moment *t*, is given by (Gaiceanu, 2002), (Athans, *et al.*, 2006)

$$u^*(t) = -\boldsymbol{R}^{-1}\boldsymbol{B}^T\boldsymbol{P}(t_1 - t)\boldsymbol{x}(t) + \boldsymbol{R}^{-1}\boldsymbol{B}^T\boldsymbol{K}_1(t_1 - t)\boldsymbol{x}_1 + \boldsymbol{R}^{-1}\boldsymbol{B}^T\boldsymbol{K}_2(t_1 - t)\boldsymbol{w}(t) \tag{37}$$

in which $\mathbf{P(t_1\text{-}t)}$ is the solution of the matrix Riccati differential equation, MRDE, and the matrices K_1 and K_2 are calculated via $P(t_1\text{-}t)$ (Rosu, *et al.*, 1998).

The numerical solution supposes the knowledge of the disturbance $\mathbf{w}(t)=T_L(t)$, which could be available by using torque estimator, as in (Rosu, *et al.*, 1998), or with torque sensor (more expensive solution that can produce the faults of the electrical drive system).

4. Simulation and experimental results

In order to implement the optimal control system two electrical drive systems are combined: the conventional vector control and the optimal control drive. Both electrical drive systems operate in parallel. The activation of one of them depends on the speed error: *if* the speed error is zero (steady state operating regime), *then* the *conventional vector control* is active, *else* the *optimal control* drive is active.

4.1. Optimal control implementation

Optimal control implementation consists of loading nine software modules developed by the author: nameplate motor data (Fig.1), determination of the motor parameters (Appendix 1), determination of the six sectors vector components to be used in Space Vector Modulation

(SVM) (Appendix 2), standard space state form characterization of the three phase Induction Motor (Fig.2), the proper arrangement of the eigenvalues and eigenvectors (Appendix 3), optimal control implementation in MATLAB (Appendix 4), the main program (Appendix 5), graphical representation (Appendix 6), Space Vector Modulation –Matlab function **svm_mod** (Appendix 7). By using the Matlab code from Appendix 8 the graphical representation of the simulation results can be obtained (Figures 4-7).

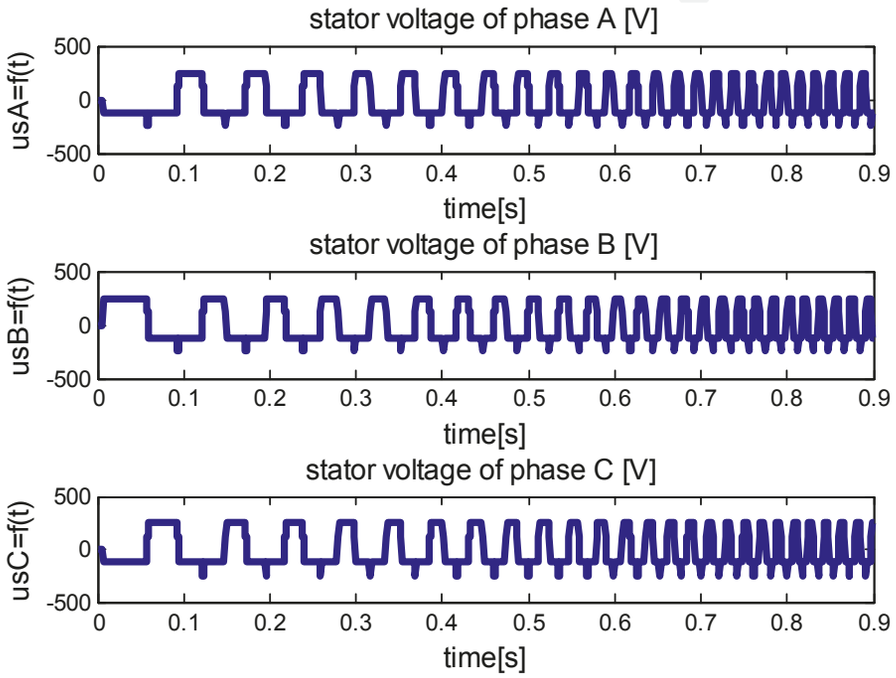

Figure 4. Three phase SVM supply voltages

Remark

The SVM increases the DC-link voltage usage, the maximum output voltage based on the space vector theory is $2/\sqrt{3}$ times higher than conventional sinusoidal modulation (Pulse Width Modulation). The purpose of the SVPWM technique is to approximate the reference voltage vector U_{out} by a combination of the eight switching patterns. The implemented Matlab sequence for obtaining the pulse pattern of the optimal SVM modulator (Appendix 2, Appendix 7) shown above is based on the developed methodology by the author (Gaiceanu, 2002). In optimal control case, there is no speed overshoot, and smoothly state response (speed and angle of the rotor magnetizing current) have been obtained (Fig.5, Fig.7).

http://dx.doi.org/10.5772/57521

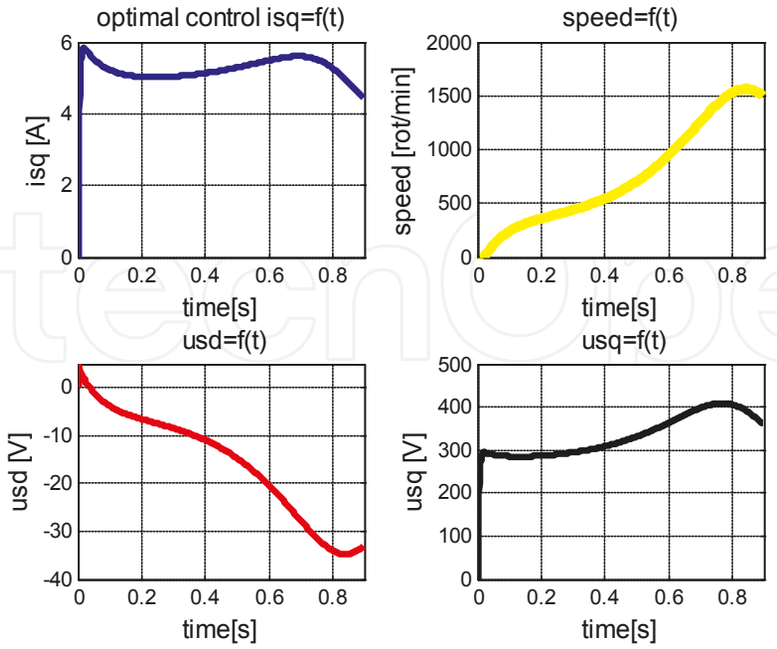

Figure 5. Optimal control, speed, longitudinal and transversal voltage components

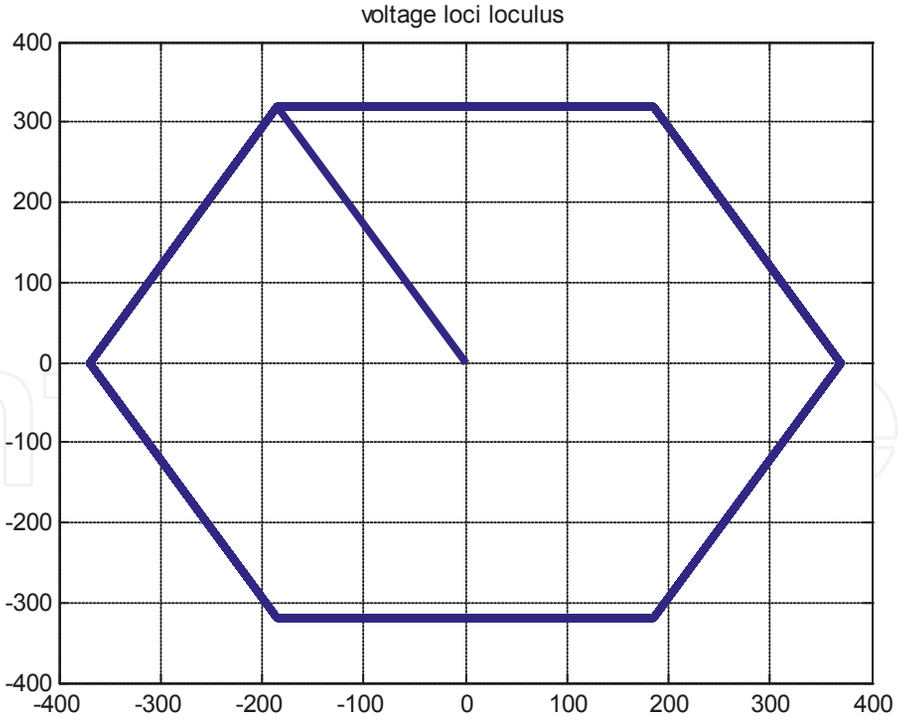

Figure 6. Voltage loci loculus for a starting process

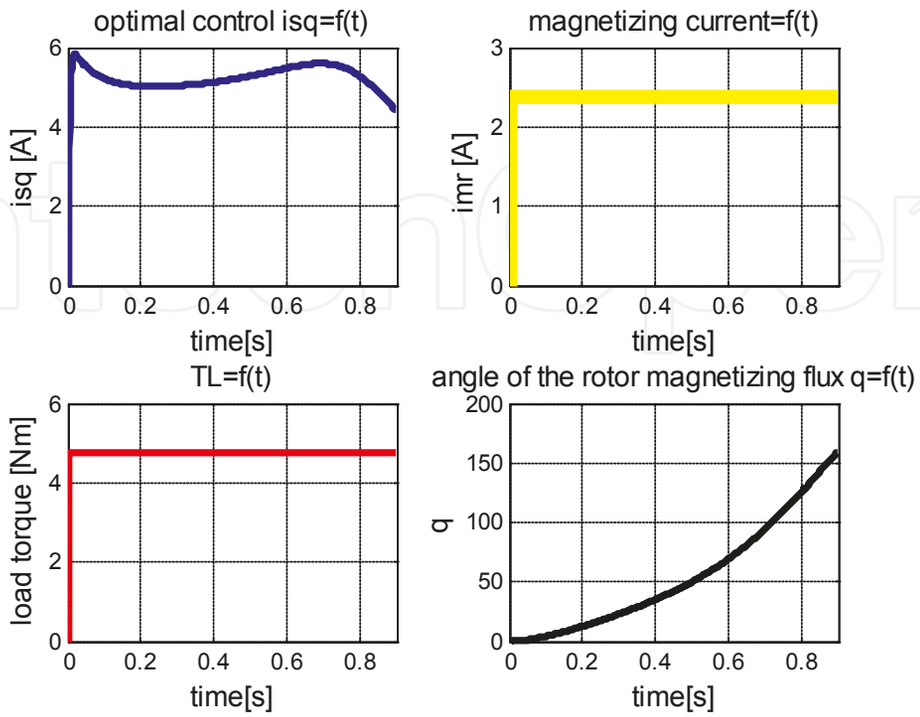

Figure 7. Optimal control $i_{qs}=f(t)$, current $i_{mr}(t)$, load torque $T_L(t)$(elevator), rotor magnetizing angle of the rotor field $q(t)$ (left to right)

4.2. Conventional vector control

The conventional vector control consists of the rotor flux orientated drive system. The vector control is implemented in Simulink as following. The control system is in cascaded manner and consists of two major loops: the speed loop and the magnetic flux loop. The torque control loop is the minor loop of the speed control one. The references of the control loop are: the desired angular velocity for the speed loop, ω^*, the imposed stator current torque component for the torque loop, i^*_{qs}, and the desired stator current flux component for the magnetization flux loop, i^*_{ds}.

Tuning of the speed and flux controllers

By knowing the nameplate motor data (Fig.1), the tuning of the PI speed and flux controllers parameters can be done (see the developed Matlab file shown in the Appendix 8). The conventional vector control supposes the use of the two independent control axes: *d*-axis, along with the magnetizing flux direction, and *q* axis, in quadrature with *d*-axis. The most used field orientated control is that of the rotor orientated magnetizing flux (Fig.8). The magnetization flux and the torque can be controlled independently.

http://dx.doi.org/10.5772/57521

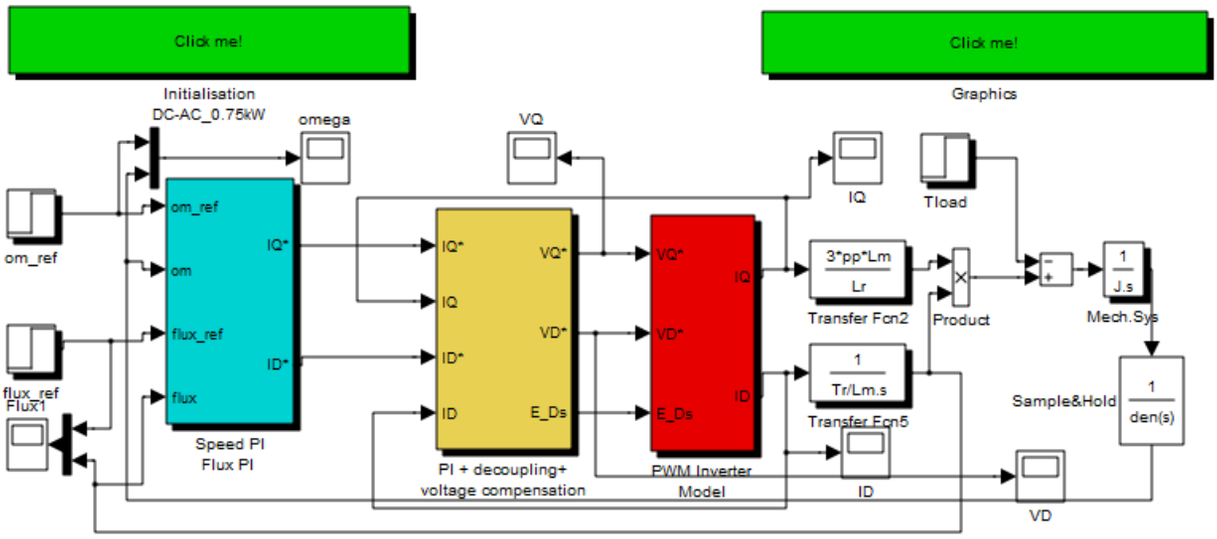

Figure 8. Simulink implementation of the rotor field orientated vector control of the three-phase induction motor

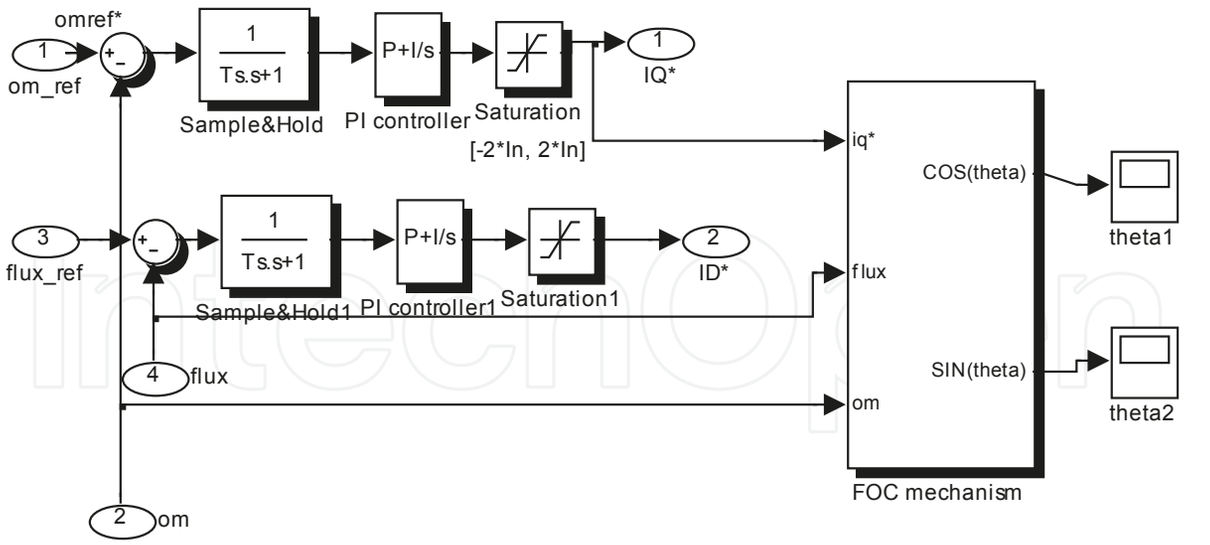

Figure 9. Simulink implementation of the speed and flux Proportional-Integral (PI) regulators

The inputs of the speed and flux regulators Simulink block (Fig.9) are the speed reference and the flux reference; the outputs are the *q*-axis reference current, IQ*, and *d*-axis reference current, ID*(Fig.10). More details can be obtained by using Fig. 10.

The inputs of the speed and flux regulators Simulink block (Fig.9) are speed refere
the flux reference; the outputs are: the *q*-axis reference current, IQ*, and *d*-axis re
current, ID*(Fig.10). More details can be obtained by using Fig. 10.

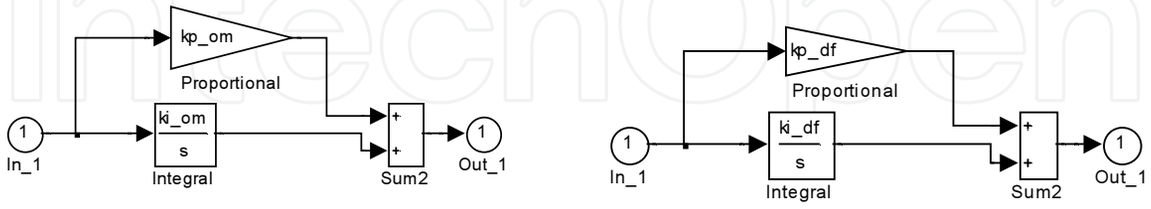

Figure 10. PI Speed regulator of type1 (kp_om+ki_om/s) and Flux regulator of type 3 (kp_df+ki_df/s), according to Matlab file shown in the Appendix 8.

Figure 10. PI Speed regulator of type1 (kp_om+ki_om/s) and Flux regulator of type 3 (kp_df+ki_df/s), according to Matlab file shown in the Appendix 8

By using the field orientated mechanism implemented in Simulink (Fig.11), based on the input signals (IQ*, *flux* and *om*), the frequency of the stator voltage is delivered.

By using the field orientated mechanism implemented in Simulink (Fig.11), based
input signals (IQ*, *flux* and *om*), the frequency of the stator voltage is delivered.

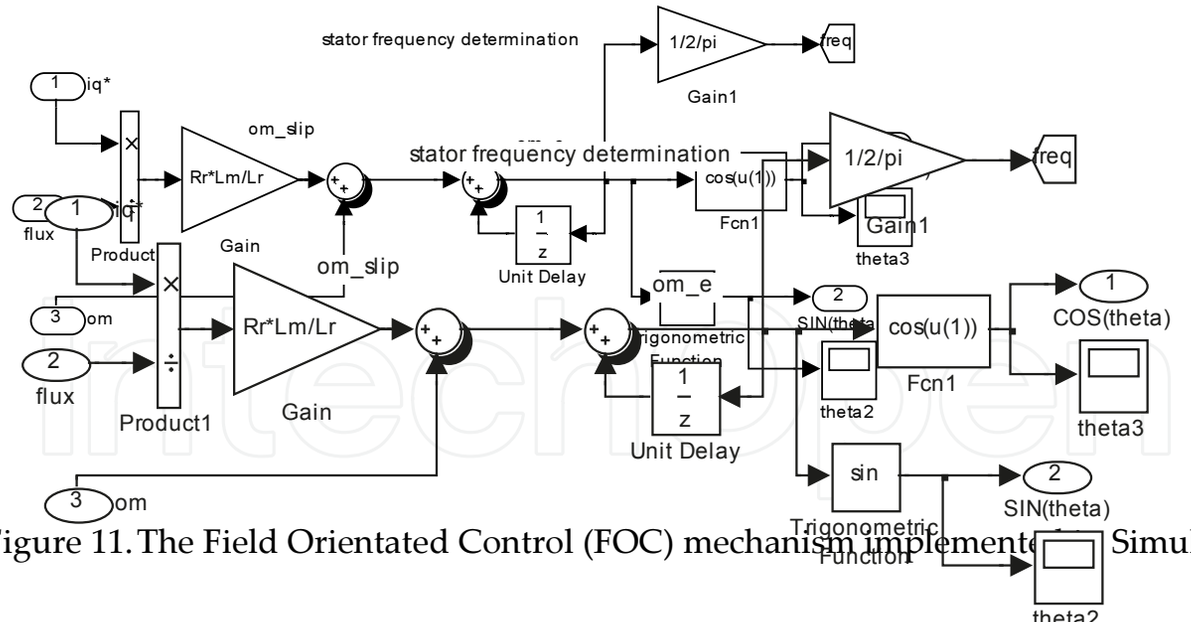

Figure 11. The Field Orientated Control (FOC) mechanism implemented in Simulink.

The parameters of the speed and flux regulators are delivered by using the Ma
developed in the Appendix 8.

Figure 11. The Field Orientated Control (FOC) mechanism implemented in Simulink

http://dx.doi.org/10.5772/57521

The parameters of the speed and flux regulators are delivered by using the Matlab file developed in the Appendix 8.

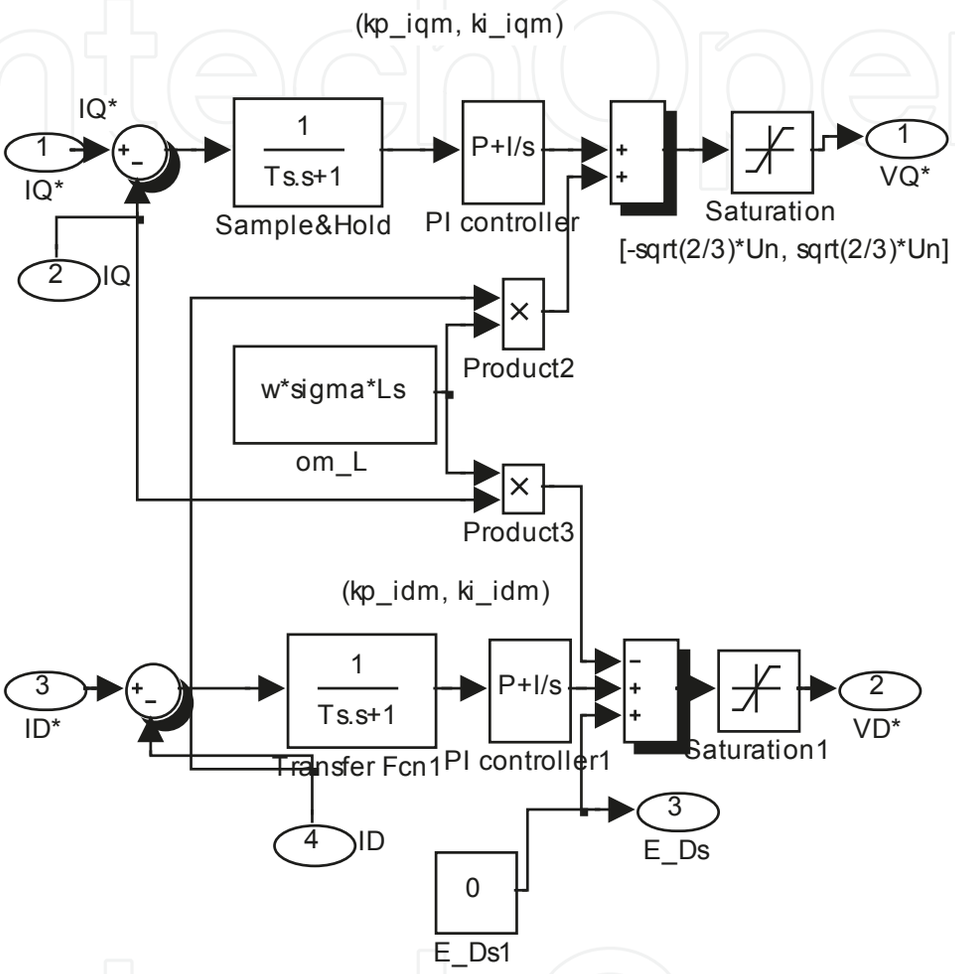

Figure 12. Detailed program of the PI control (torque (IQ*) and flux (ID*) control loops), the decoupling of the *d*, *q* axes, and the voltage compensation Simulink block of Fig.7

In the Fig.12. the detailed decoupling and the voltage compensation between *d*, *q* axes are depicted. In order to control the torque current component (IQ) and the flux current component (ID), the PI controllers are involved. By introducing the compensating voltage components, the independent control of flux and torque is obtained (Fig.12).

The reference voltage components pair (VD*, VQ*) is used as input of the Pulse Width Modulation (PWM) transfer function block, shown in the Fig.13.

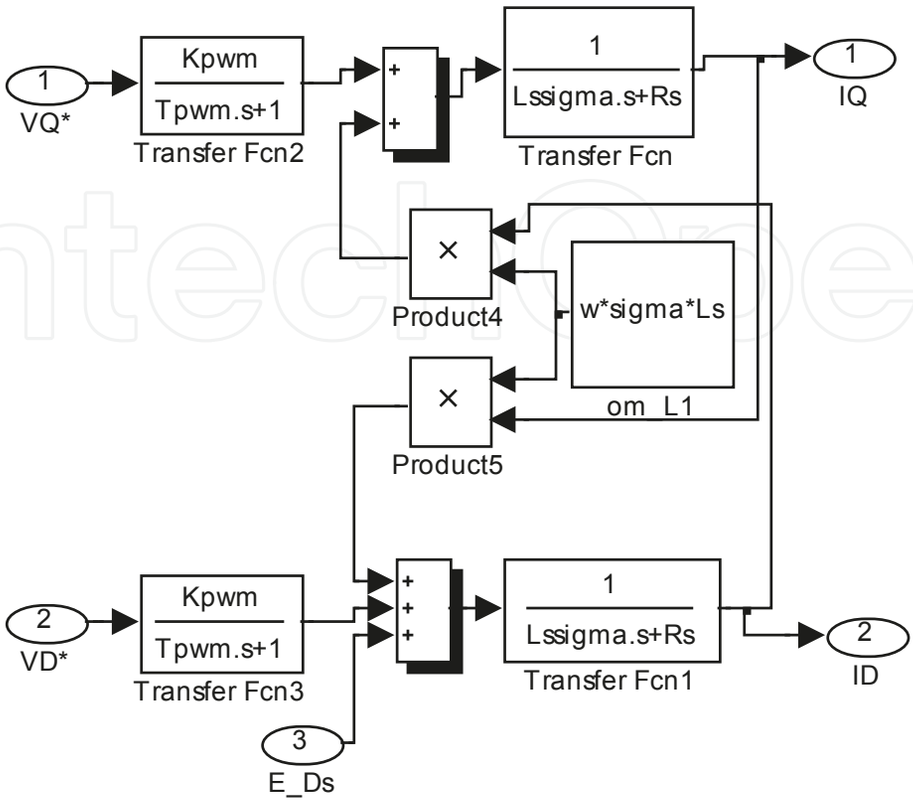

Figure 13. The Simulink models of the PWM modulator and of the equivalent *d*, *q* model of the IM

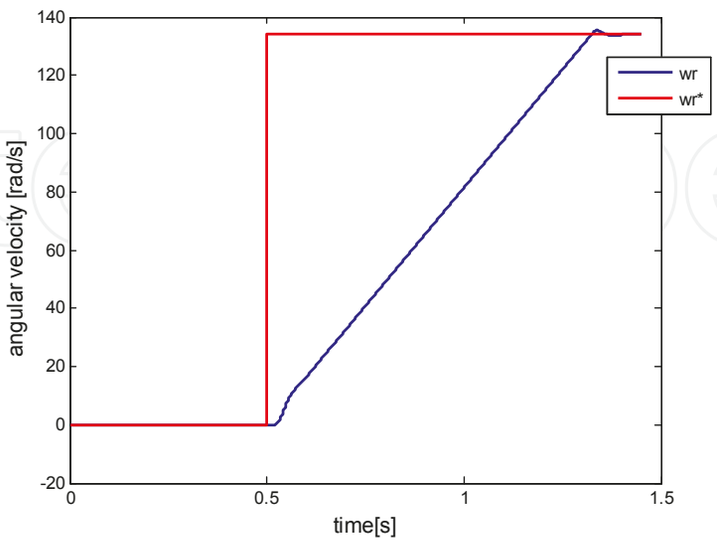

Figure 14. The speed control loop

http://dx.doi.org/10.5772/57521

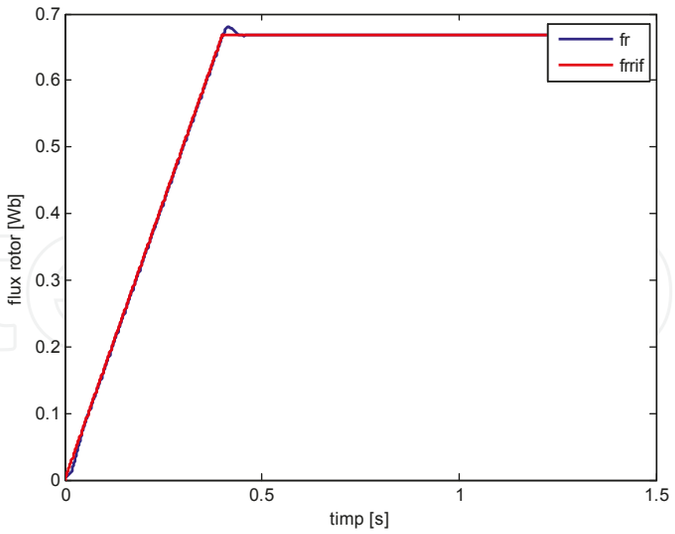

Figure 15. The rotor flux control loop

The performances of the speed control loop are shown in the Fig. 14, in which the step rotor speed reference (om_ref*) is applied and the actual rotor speed (om) follows the reference with zero steady state error. The performances of the implemented flux control loop are shown in the Fig. 15. Small flux overshoot (up to 11%) and zero steady state error are obtained (Fig.15). The IM starts after *t*=0,5s (Fig.15), when the rated flux of the motor is attained (Fig.15). In order to implement the optimal control for ac drives, a test bench based on the DS1104 platform has been developed (Fig.16).

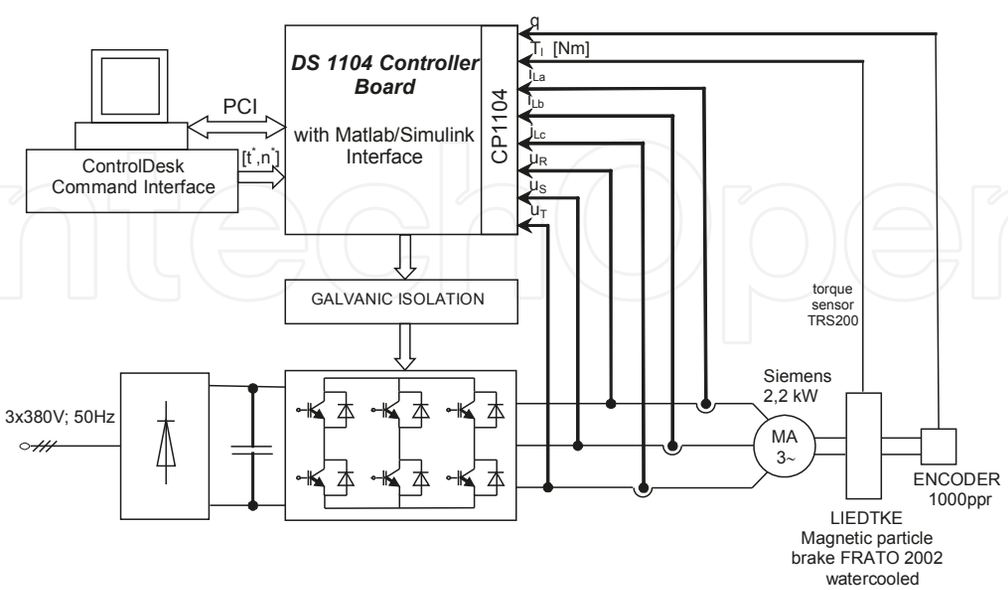

Figure 16. The experimental set-up test bench (Gaiceanu *et al*., 2008)

Figure 16. The experimental set-up test bench (Gaiceanu *et al.*, 2008).

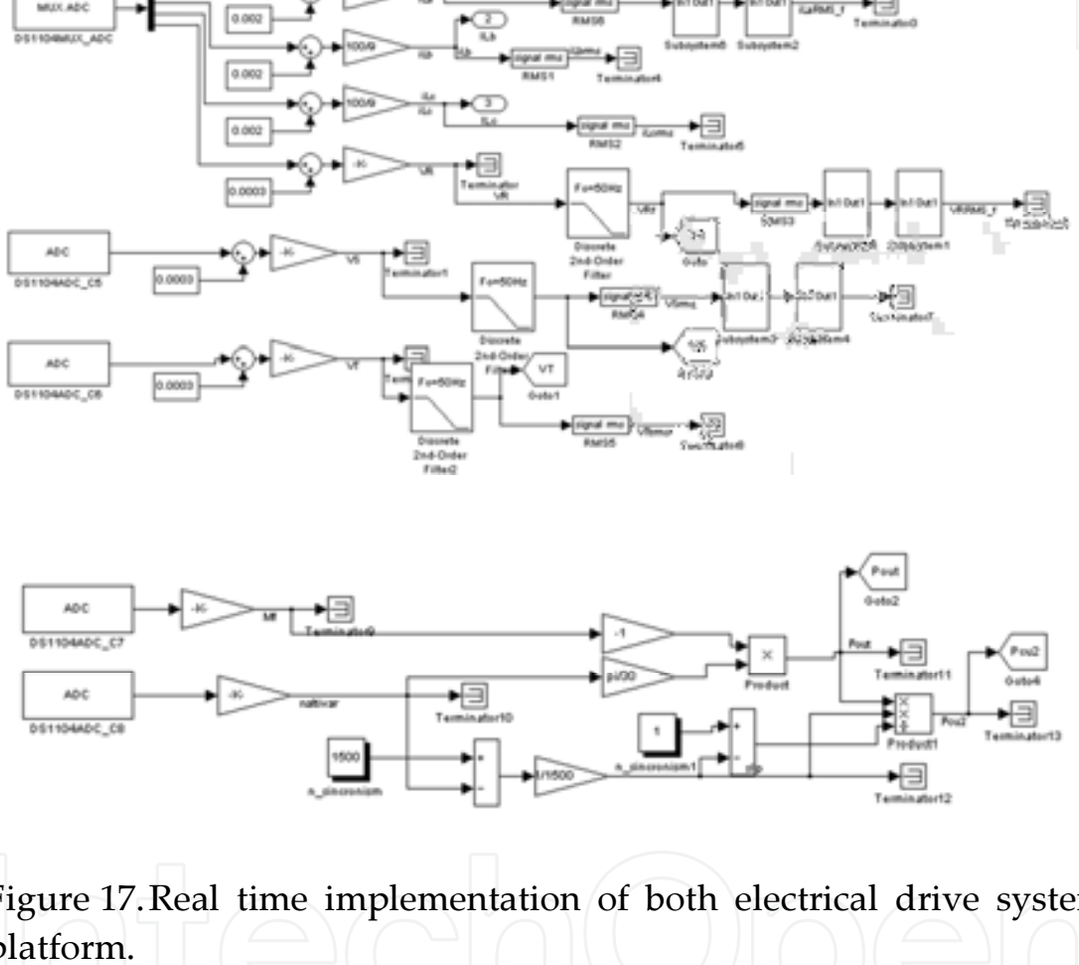

Figure 17. Real time implementation of both electrical drive systems based on the DS1104 platform.

Figure 17. Real time implementation of both electrical drive systems based on the DS1104 platform.

Both types of control, i.e. conventional and optimal, have been implemented on DS1104 (Fig. 17) controller board. The developed ControlDesk interface has two main functions: real time control and signals acquisition. The evaluation of the obtained experimental results reveals the system efficiency improvement through an important decreasing of the windings dissipation power and input power (Fig.18) in optimal control case. Therefore, the power balance provides an increasing of the system efficiency, thus improved thermal and capacity conditions are obtained.

The optimal control (7) of the electrical drive based on the induction mach numerically simulated by using Z transform and zero order hold for a s [kW], 1480 [rpm] under a rating load torque of 4.77 [Nm]. The initial conditio control problem are: t_o=0[s], $\mathbf{x}_i$=[n_i=0 q=0]. The free final conditions are: t_f=

http://dx.doi.org/10.5772/57521

The optimal control (7) of the electrical drive based on the induction machine (1) has been numerically simulated by using Z transform and zero order hold for a starting of a 0.75 [kW], 1480 [rpm] under a rating load torque of 4.77 [Nm]. The initial conditions of the optimal control problem are: t_o=0[s], $\mathbf{x}_i$=[n_i=0 q=0]. The free final conditions are: t_f=0.9[s], $\mathbf{x}_f$=[n_f=1480 q=0].

5. Conclusions

In order to obtain the optimal control, the nonrecursive solution has been used to avoid the main disadvantages of the recursive solution (that is, the solution can be calculated at the current time, not backward in time; the load torque can have any shape, either linear or nonlinear, in admissible limits, due to the fact that the solution is computed at each sample time).

A simplified solution is proposed by avoiding the constrained optimal control problem type. By using an adequate weighting matrices **S**, **R** and **Q**, the magnitude constraints have been solved. In this way the states and the control signals are maintained in admissible limits.

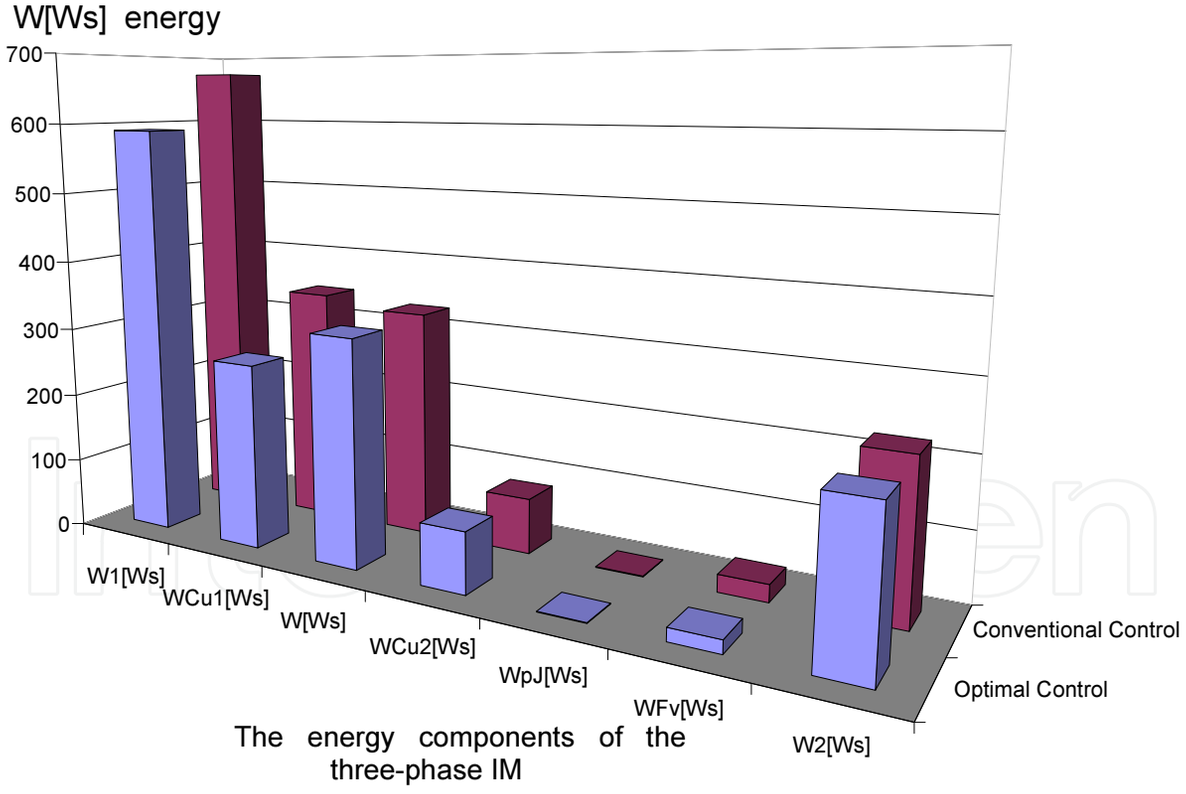

Figure 18. Conventional and optimal control: comparative evaluation of the energy.

The optimal problem shown in this chapter has been formulated for a starting period. In the Fig.18, the energy evaluation for both control methods, conventional and optimal, is depicted. According to Bellman's theorem of optimality, the optimal problem can be extended also on the braking, or reversing periods. The components of the energy of the three-phase IM (Fig.20) are: W_1 the input energy, W_2 the output energy, W_{Cu1} the energy expended in the stator windings, W_{Cu2} the energy expended in the rotor windings, W_{Fv} the viscous friction dissipated energy, W_{pJ} the accumulated energy in inertial mass, W the electromagnetic energy.

Figure 18. Conventional and optimal control: comparative evaluation of the energy

From energetic point of view it could be noticed that the output energy is the same in both

A simplified solution is proposed by avoiding the constrained optimal control problem type. By using adequate weighting matrices **S**, **R** and **Q**, the magnitude constraints have been solved. In this way the states and the control signals are maintained in admissible limits.

The optimal problem shown in this chapter has been formulated for a starting period. In the Fig.18, the energy evaluation for both control methods, conventional and optimal, is depicted. According to Bellman's theorem of optimality, the optimal problem can be extended also on the braking, or reversing periods. The components of the energy of the three-phase IM (Fig. 20) are: W_1 the input energy, W_2 the output energy, W_{Cu1} the energy expended in the stator windings, W_{Cu2} the energy expended in the rotor windings, W_{Fv} the viscous friction dissipated energy, W_{pJ} the accumulated energy in inertial mass, W the electromagnetic energy.

From the energetic point of view, it could be noticed that the output energy is the same in both controls (conventional and optimal) while the input energy decreases significantly in the optimal control case due to the decreasing of the stator copper losses, even if the rotor losses slightly increase in the optimal control case (Fig.20).

The proposed optimal control conducts to 8% electrical energy reduction, despite of using the conventional control. The conclusion is: decreasing the input energy for the optimal control system at the same time with maintaining the output energy in both systems, classical and optimal, the efficient electric drive system is obtained.

Due to using only the negative exponentials terms, the system is stable.

The optimal control can be applied in the applications with frequent dynamic regimes. The minimization of the consumed energy conducts to an increasing of the operational period of the electrical drives, or to the electrical motor overload allowance.

The optimal control could be extended to the high phase order induction machine applications, in a decoupled *d-q* rotor field oriented reference frame and by using adequate control of the power inverter (Gaiceanu, 2002).

Taking into consideration that this chapter is focused on developing and proving the performances of the optimal Electrical Drive Systems (EDS), an immediate effect is represented by the positive impact on the market as an alternative for electrical efficiency. The key of the proposed chapter is the integration of the developed Matlab tool by means of the high technology, i.e. the development of the systems with microprocessor. The chapter leads to drawing up specific research and development methods in the field of electrical drives. It has been underlined that by making EDS in an efficient manner, the CO2 emission reduction will be also obtained.

The achievement of this chapter is the opportunity to attract young MSc. and PhD students in R&D activities that request both theoretical and practical knowledge. The author will have new opportunities for developing international interdisciplinary research, technological transfer, sharing of experience and cooperation in the framework of the specific Research Programmes.

http://dx.doi.org/10.5772/57521

Appendix 1

```
%%%%%%%%%%%%%%%%%%%%%%%%%%%%%%%%%%%%%%%%%%%%%%%%%%%%%%%%%
% Parameters determination of the three-phase squirrel cage induction motor %
%  Developed by Marian Gaiceanu                                              %
%%%%%%%%%%%%%%%%%%%%%%%%%%%%%%%%%%%%%%%%%%%%%%%%%%%%%%%%%
%syncronism speed
 n=60*f1/p;     %[rot/min]
%rated electromagnetic torque
 Mn=9550*P*10^(-3)/n; %[Nm]
%rated load torque
 Mr=Mn;     %[Nm]
%pulsation of the supply voltage
 om1=2*pi*f1; %[rad/sec]
%power factor
 cosfi=0.71;
 %rated efficiency
 etan=0.794;
 %rated speed
 nn=1480;
 %syncronism speed
 n=60*f1/p;     %[rot/min]
 %total inductance
 Ls=Lss+Lm;   %[H]
%rotor inductance
 Lr=Lrs+Lm;   %[H]
%stator time constant
 Ts=Ls/Rs;    %[sec]
%rotor time constant
Tr=Lr/Rr;    %[sec]
%Total leakage factor
sinfi=sqrt(1-cosfi^2);
sigmav=(1-cosfi)/(1+cosfi)
sigma=sigmav
sigmar=Lr/Lm;
%Nominal voltage and nominal frequency of the supply voltage
Un=380;fn=f1;
%rated stator current
In=P/(sqrt(3)*Un*cosfi*etan)
%Nominal magnetizing current
Im=sqrt(sigmav)*In
%Load current Iq=Itorque
It=sqrt(In^2-Im^2)
%Rated flux
lambda_nom=sqrt(1-sigmav)*Un/(sqrt(3)*2*pi*fn) %[Wb]
%number of pole pairs
p=fn*60/n
%nominal slip
sn=n-nn
%Electrical power of the motor
Peln=P/etan
%Torque constant -check point
kt=3*p*lambda_nom/(1+sigmav)%Nm/A
%magnetizing current
Im=lambda_nom/Lm; %A
%inductivitatea de scapari statorica
Lssigma=sigmav*Un/(sqrt(3)*2*pi*fn*Im)
%Rotor approximated inductance
Lr1=(1+sigmav)*Lm  %H
Lrs=Lr1;
%Stator inductance
Lsv=Lssigma/sigmav
Ls1=(1+sigmav)*Lm
Lss=Ls1;
%rotor inductance
Lrv=Lm^2/(Lsv*(1-sigmav))
%d-axis reference stator current
Idref=lambda_nom/Lm
%variable frequency initialization
i=2;%
t0=0.001;%sampling period [s].
t=t0;
q=0; om=0;
tf=0.9;%fixed final time [s] from Fig. 15., conventional control
fi=50; omi=2*pi*fi;
omv=0; tfomv=tf;
imr=Idref;
isd=imr;
```

Appendix 2

```
%%%%%%%%%%%%%%%%%%%%%%%%%%%%%%%%%%%%%%%%%%%%%%%%%%%%%%%%%%%%%
% vector components of six sectors for using in Space Vector Modulation -SVM (Appendix 6)    %
% Parameters determination of the three-phase squirrel cage induction motor                  %
% Developed by Marian Gaiceanu                                                               %
%%%%%%%%%%%%%%%%%%%%%%%%%%%%%%%%%%%%%%%%%%%%%%%%%%%%%%%%%%%%%
% Space Vector Modulation PWM: initialization
Tpwm=1/20000; % PWM cycle period
f=50;
oMfaze=2*pi*f;
Tpark=2/3*[1 -1/2 -1/2
           0 sqrt(3)/2 -sqrt(3)/2];
Vd=370; % DC link voltage
% switching/ commutation matrix
Mfaze=[2 -1 -1
   -1 2 -1
   -1 -1 2];
Mfaze=Mfaze*Vd/3;
% 1st vector
global U0_alpha U0_beta
a=1; b=0; c=0;
Vabc=Mfaze*[a b c]';
U0=Tpark*Vabc;
U0_alpha=U0(1,1);
U0_beta=U0(2,1);
% 2nd vector
global U60_alpha U60_beta
a=1; b=1; c=0;
Vabc=Mfaze*[a b c]';
U60=Tpark*Vabc;
U60_alpha=U60(1,1);
U60_beta=U60(2,1);
% 3rd vector
global U120_alpha U120_beta
a=0; b=1; c=0;
Vabc=Mfaze*[a b c]';
U120=Tpark*Vabc;
U120_alpha=U120(1,1);
U120_beta=U120(2,1);
% 4th vector
global U180_alpha U180_beta
a=0; b=1; c=1;
Vabc=Mfaze*[a b c]';
U180=Tpark*Vabc;
U180_alpha=U180(1,1);
U180_beta=U180(2,1);
% 5th vector
global U240_alpha U240_beta
a=0; b=0; c=1;
Vabc=Mfaze*[a b c]';
U240=Tpark*Vabc;
U240_alpha=U240(1,1);
U240_beta=U240(2,1);
% 6th vector
global U300_alpha U300_beta
a=1; b=0; c=1;
Vabc=Mfaze*[a b c]';
U300=Tpark*Vabc;
U300_alpha=U300(1,1);
U300_beta=U300(2,1);
%Fig.2
%State space model
```

http://dx.doi.org/10.5772/57521

Appendix 3

```
%%%%%%%%%%%%%%%%%%%%%%%%%%%%%%%%%%%%%%%%%%%%%
% The proper arrangement of the eigenvalues and eigenvectors %
% Developed by Marian Gaiceanu                              %
%%%%%%%%%%%%%%%%%%%%%%%%%%%%%%%%%%%%%%%%%%%%%
% Weighting matrices

  S=[100  0;
     0  0];
  Q=[1*J/1  0;
    0    0.001 ];
  R=[0.08] ;
%bloc optimal
%the matrix of the canonical system
M=[-A  B*inv(R)*B';
       Q    A']
%eigenvectors and eigenvalues
[v,d]=eig(M);
vecinit=v;
valnit=d;
%   the   arrangements   of   the   eigenvalues   and   of   the   corresponding   eigenvectors   on   the   diagonal   matrix   D
% in order to obtain only the negative eigenvalues
val=[d(1,1) d(2,2) d(3,3) d(4,4)];
x=sort(val);
if x(1,4)==d(2,2),
  aux0=d(2,2);
  d(2,2)=d(1,1);
  d(1,1)=aux0;
  aux9=v(:,2);
  v(:,2)=v(:,1);
  v(:,1)=aux9;
 elseif x(1,4)==d(3,3),
  aux1=d(3,3);
  d(3,3)=d(1,1);
  d(1,1)=aux1;
  aux2=v(:,3);
  v(:,3)=v(:,1);
  v(:,1)=aux2;
elseif x(1,4)==d(4,4),
  aux3=d(4,4);
  d(4,4)=d(1,1);
  d(1,1)=aux3;
  aux4=v(:,4);
  v(:,4)=v(:,1);
  v(:,1)=aux4;
end
if x(1,3)==d(3,3),
  aux5=d(3,3);
  d(3,3)=d(2,2);
  d(2,2)=aux5;
  aux6=v(:,3);
  v(:,3)=v(:,2);
  v(:,2)=aux6;
elseif x(1,3)==d(4,4),
  aux7=d(4,4);
  d(4,4)=d(2,2);
  d(2,2)=aux7;
  aux8=v(:,4);
  v(:,4)=v(:,2);
  v(:,2)=aux8;
end
if x(1,1)==d(4,4),
  aux10=d(4,4);
  d(4,4)=d(3,3);
  d(3,3)=aux10;
  aux11=v(:,4);
  v(:,4)=v(:,3);
  v(:,3)=aux11; end
W=v ; %the eigenvectors
D=d; %the eigenvalues
```

Appendix 4

```
%%%%%%%%%%%%%%%%%%%%%%%%%%%%%%%%
% Optimal control implementation in MATLAB  %
% Developed by Marian Gaiceanu                          %
%%%%%%%%%%%%%%%%%%%%%%%%%%%%%%%%
%  checking point of eigenvalues and eigenvectors
   Dv=inv(W)*M*W;
%   the eigenvalues
   lambda=diag(D);
%   Matrix -(lambda)
   mlambda=[D(3,3) D(3,4);
            D(4,3) D(4,4)];
%   submatrices of the eigenvectors
   W11=[W(1,1) W(1,2);
        W(2,1) W(2,2)];
   W12=[W(1,3) W(1,4);
        W(2,3) W(2,4)];
   W21=[W(3,1) W(3,2);
        W(4,1) W(4,2)];
   W22=[W(3,3) W(3,4);
        W(4,3) W(4,4)];
%   the inverse of the eigenvectors matrix
   W1=inv(W);
%   extension of the perturbation vector G
   G1=[G;0;0];
   Gp=W1*G1;
   H= Gp./lambda;
   H1=[H(1,1);
      H(2,1)];
   H2=[H(3,1);
      H(4,1)];
   I1=inv(S*W12-W22);
   E=I1*(W21-S*W11);
   F=I1*S;
   xi=[0;0];     %initial conditions  (state vector) for a starting
   xf=[n,0]; tau=tf; % final conditions for a starting: final state and final time
   Yi3=0;    Yif3=[0;0];% initial value for the filter matrices
   Ii=eye(2);    % [2x2] identity matrix I2
   wp=Mr;       % initial perturbation value
   Ta=0.07;      % filter time constant
   swcu=0;
   kq=1/Tr/imr; % IM torque constant
yc1=exp(-t0/Ta);   yc2=1-yc1; c1=exp(-t0*Fv/J); c3=(1-c1)/Fv;
```

http://dx.doi.org/10.5772/57521

Appendix 5

```
%%%%%%%%%%%%%%%%%%%%%%%%%%%%%%%%%
% Main Program                                        %
% Developed by Marian Gaiceanu                             %
%%%%%%%%%%%%%%%%%%%%%%%%%%%%%%%%%
while (t<=tf)&(tau>0),
     tau=tf-t;
     emlamt=expm(mlambda*tau);
     Z=emlamt*E*emlamt;
     P=(W21+W22*Z)*(inv(W11+W12*Z));
     V=W22-P*W12;
     Iie=Ii-emlamt;
     T=V*(emlamt*E*Iie*H1+Iie*H2);
     K=V*emlamt*F;
   %
     Yi1=-inv(R)*B'*(P*xi);
     Yiw=Yi3*exp(-t0/Ta)+wp*(1-exp(-t0/Ta));
     Yi4=-inv(R)*B'*(T*Yiw);
     Yif=Yif3*exp(-t0/Ta)+xf*(1- exp(-t0/Ta));
     Yi2=-inv(R)*B'*(K*Yif);
     %comanda optima
     isq(i)=Yi1+Yi2+Yi4;
     isqo=isq(i-1);%therefore i=2 as initialization;
  %mathematical model
  % d, q supply voltage components
   usd(i)=Rs*isd*(1-sigma*Ts*(om+isqo*kq));
   usq(i)=Rs*(sigma*Ts*isq(i)/t0-isqo*(-1+(sigma-1)*Ts*imr*kq+sigma*Ts*isd*kq)-om*(sigma*Ts*isd+Ts*(sigma-1)*imr));
   Me(i)=p*km*imr*isq(i); %electromagnetic torque
   %electrical speed
  omu(i)=om*exp(-t0*Fv/J)+p*(Me(i)-wp)*(1- exp(-t0*Fv/J))/Fv;
   %rotor (mechanical) speed
  nr(i)=30*omu(i)/pi/p;
   %load torque variation limits
    if t>0,
      wp=1*Mr;
    else
      wp=0*Mr;
    end
  wpr(i)=wp;
  % angle of the rotor magnetization current vector, imr
  qu(i)=q+t0*(omu(i)+isq(i)/(Tr*imr));

   % data refreshing
   xi=[nr(i);qu(i)];
   Yi3=Yiw; Yif3=Yif;
  isalfa=cos(qu(i))*isd-sin(qu(i))*isq(i);
  isbeta=sin(qu(i))*isd+cos(qu(i))*isq(i);
  isa(i)=2*isalfa/3;
  isb(i)=-isalfa/3+isbeta/sqrt(3);
  isc(i)=-isalfa/3-isbeta/sqrt(3);
%three phase supply stator voltages
usalfa=cos(qu(i))*usd(i)-sin(qu(i))*usq(i);
V_alpha=usalfa;
usbeta=sin(qu(i))*usd(i)+cos(qu(i))*usq(i);
V_beta=usbeta;
ualfas(i)=usalfa;
ubetas(i)=usbeta;
% Space Vector Modulation
[Va Vb Vc]=svm_mod(Vd,V_alpha,V_beta,t,Tpwm);
   usa(i)=2*usalfa/3;
   usb(i)=-usalfa/3+usbeta/sqrt(3);
   usc(i)=-usalfa/3-usbeta/sqrt(3);
   ualfas1(i)=usalfa;
   ubetas1(i)=usbeta;
   V_alfar=Va-(1/2)*Vb-(1/2)*Vc;
   ualfar(i)=V_alfar;
   V_betar=(sqrt(3)/2)*Vb-(sqrt(3)/2)*Vc;
   ubetar(i)=V_betar;
   udr=cos(qu(i))*V_alfar-sin(qu(i))*V_betar;
   uqr=sin(qu(i))*V_alfar+cos(qu(i))*V_betar;
t=t+t0;            tplot(i)=t;            Vaplot(i)=Va;            Vbplot(i)=Vb;            Vcplot(i)=Vc;    imru(i)=imr;    isdu(i)=isd;    isqi(i)=isqo;
q=qu(i);  om=omu(i); i=i+1;
end
```

Appendix 6

Appendix 6

```
%%%%%%%%%%%%%%%%%%%%%%%%%%%%%%%%%%%%
% Graphical representation                %
% Developed by Marian Gaiceanu            %
%%%%%%%%%%%%%%%%%%%%%%%%%%%%%%%%%%%%
figure(1)
subplot(3,1,1)
plot(tplot,Vaplot,'LineWidth',3)
ylabel('usA=f(t)','FontSize',12)
    xlabel('time[s]','FontSize',12)
    title('stator voltage of phase A [V]','FontSize',12)
axis([0 .9 -500 500])
subplot(3,1,2)
plot(tplot,Vbplot,'LineWidth',3)
ylabel('usB=f(t)','FontSize',12)
    xlabel('time[s]','FontSize',12)
    title('stator voltage of phase B [V]','FontSize',12)
axis([0 .9 -500 500])
subplot(3,1,3)
plot(tplot,Vcplot,'LineWidth',3)
ylabel('usC=f(t)','FontSize',12)
    xlabel('time[s]','FontSize',12)
    title('stator voltage of phase C [V] ','FontSize',12)
axis([0 .9 -500 500])

figure(2)
    t=0:t0:tf-2*t0;
    i=1:1:length(t);
    subplot(2,2,1);
    plot(t,isq(i),'k','LineWidth',3);
    title('optimal control isq=f(t)','FontSize',12)
    xlabel('time[s]','FontSize',12)
    ylabel('isq [A]','FontSize',12)
    grid
    axis([0 0.9 0 6])
subplot(2,2,2);
    plot(t,nr(i),'k','LineWidth',3);%omu(i)
    title('speed=f(t)','FontSize',12)
    xlabel('time[s]','FontSize',12)
    ylabel('speed [rot/min]','FontSize',12)
    grid
    axis([0 0.9 0 2000])

    subplot(2,2,3);
plot(t,usd(i),'k','LineWidth',3);
    title(' usd=f(t)','FontSize',12)
    xlabel('time[s]','FontSize',12)
    ylabel('usd [V]','FontSize',12)
    grid
    axis([0 0.9 -40 5])
    subplot(2,2,4);
    plot(t,usq(i),'k','LineWidth',3);
    title(' usq=f(t)','FontSize',12)
    xlabel('time[s]','FontSize',12)
    ylabel('usq [V]','FontSize',12)
    grid
    axis([0 0.9 0 400])
figure(3)
     t=0:t0:tf-2*t0;
    i=1:1:length(t);
    plot(ualfas1(i),ubetas1(i),'b','LineWidth',3)
    title('stator voltage loci loculus')
   xlabel('ualfa[V]')
   ylabel('ualbeta [V]')
   grid;
figure(4)
     t=0:t0:tf-2*t0;
    i=1:1:length(t);
    plot(ualfar(i),ubetar(i),'b','LineWidth',3);
    title('voltage loci loculus')
   grid;
```

http://dx.doi.org/10.5772/57521

Appendix 7

```
%%%%%%%%%%%%%%%%%%%%%%%%%%%%%%%%%%%%%%%%%%%%%
% Space Vector Modulation implemented as a Matlab function %
% Developed by Marian Gaiceanu                %
% svm_mod (Vd,V_alpha,V_beta,t,Tpwm)          %
%%%%%%%%%%%%%%%%%%%%%%%%%%%%%%%%%%%%%%%%%%%%%
%Implemented Matlab function of the Space Vector Modulation
function [Va,Vb,Vc] = svm_mod (Vd,V_alpha,V_beta,t,Tpwm)

global U0_alpha U0_beta
global U60_alpha U60_beta
global U120_alpha U120_beta
global U180_alpha U180_beta
global U240_alpha U240_beta
global U300_alpha U300_beta

% angle of the space vector
V=sqrt(V_alpha*V_alpha+V_beta*V_beta);
if V_beta >0,
  teta=acos(V_alpha/V);
else
  teta=2*pi-acos(V_alpha/V);
end
teta=teta*180/pi;

% sector selection
if teta>=0 & teta<=60
  s=1;
elseif teta>60 & teta<=120
  s=2;
elseif teta>120 & teta<=180
  s=3;
elseif teta>180 & teta<=240
  s=4;
elseif teta>240 & teta<=300
  s=5;
else
  s=6;
end

% space vector decomposition
switch s
case 1,
  V1_alpha=U0_alpha;
  V1_beta=U0_beta;
  V2_alpha=U60_alpha;
  V2_beta=U60_beta;
case 2,
  V1_alpha=U120_alpha;
  V1_beta=U120_beta;
  V2_alpha=U60_alpha;
  V2_beta=U60_beta;
case 3,
  V1_alpha=U120_alpha;
  V1_beta=U120_beta;
  V2_alpha=U180_alpha;
  V2_beta=U180_beta;
case 4,
  V1_alpha=U240_alpha;
  V1_beta=U240_beta;
  V2_alpha=U180_alpha;
  V2_beta=U180_beta;
case 5,
  V1_alpha=U240_alpha;
  V1_beta=U240_beta;
  V2_alpha=U300_alpha;
  V2_beta=U300_beta;
```

```
case 6,
  V1_alpha=U0_alpha;
  V1_beta=U0_beta;
  V2_alpha=U300_alpha;
  V2_beta=U300_beta;
end
det=V1_alpha*V2_beta-V2_alpha*V1_beta;
T1=Tpwm*(V_alpha*V2_beta-V2_alpha*V_beta)/det;
T2=Tpwm*(V1_alpha*V_beta-V_alpha*V1_beta)/det;
T0=Tpwm-T1-T2;

% switching pulse
tc=rem(t,Tpwm);
C1=0.25*T0;
C2=C1+0.5*T1;
C3=C2+0.5*T2;
patt1 = C1<=tc & tc<=Tpwm-C1;
patt2 = C2<=tc & tc<=Tpwm-C2;
patt3 = C3<=tc & tc<=Tpwm-C3;
switch s
case 1,
  puls_a=patt1;
  puls_b=patt2;
  puls_c=patt3;
case 2,
  puls_a=patt2;
  puls_b=patt1;
  puls_c=patt3;
case 3,
  puls_a=patt3;
  puls_b=patt1;
  puls_c=patt2;
case 4,
  puls_a=patt3;
  puls_b=patt2;
  puls_c=patt1;
case 5,
  puls_a=patt2;
  puls_b=patt3;
  puls_c=patt1;
case 6,
  puls_a=patt1;
  puls_b=patt3;
  puls_c=patt2;
end
Vmatrix=(1/3)*[2 -1 -1
        -1 2 -1
        -1 -1 2]*[puls_a
                  puls_b
                  puls_c]*Vd;
Va=Vmatrix(1,:);
Vb=Vmatrix(2,:);
Vc=Vmatrix(3,:);
```

http://dx.doi.org/10.5772/57521

Appendix 8

The Matlab file for tuning of the PI speed and flux controllers parameters in conventional control

```
%%%%%%%%%%%%%%%%%%%%%%%%%%%%%%%%%%%%%%%%%%%%%%%%%%%%%%%%%%%%%%%%%%%%%%%%%%%%%%%%
% Tuning of the PI speed and flux controllers parameters: Kessler variant   %
% Developed by Marian Gaiceanu                                              %
%%%%%%%%%%%%%%%%%%%%%%%%%%%%%%%%%%%%%%%%%%%%%%%%%%%%%%%%%%%%%%%%%%%%%%%%%%%%%%%%
%sampling time
Ts=0.0001; %100us
%PWM
%gain factor
Kpwm=1; %daca nu se considera marimile de la traductoare in sistem unificat de tensiuni: 10V
Tpwm=Ts/2;

%%%%%%%%%%%%%%%%%%%%%%%%%%%%%%%%%%%
% Current loop: d- axis          %
%%%%%%%%%%%%%%%%%%%%%%%%%%%%%%%%%%%

%sum of parasite (small) time constant
Teim=Ts+Tpwm;
%controller of type 1: 1+s*tau1/(s*tau2)
tau1=Lssigma/Rs
tau2=2*Teim*Kpwm/Rs
% controller of type 2: kp_idm+ki_idm/s
kp_idm=tau1/tau2
ki_idm=1/tau2 %for Pn<10kW, else:
%for perturbation rejection (Blasko)
% controller of type 3: kp(1+1/sTim)
Tim=10*Teim %Blasko
ki_idm=kp_idm/Tim %assures a damping factor D=0.707 and a bandwidth of fbanda=fs/20

%%%%%%%%%%%%%%%%%%%%%%%%%%%%%%%%%%%
%Similarly, Current loop: q- axis%
%%%%%%%%%%%%%%%%%%%%%%%%%%%%%%%%%%%
kp_iqm=kp_idm;
ki_iqm=ki_idm;

%%%%%%%%%%%%%%%%%%%%%%%%%%%
%Speed control loop      %
%%%%%%%%%%%%%%%%%%%%%%%%%%%
%from the closed loop current transfer function
Ttm=2*Teim
%time delay constant of the sample and hold device
Tdt=Ts;
%sum of the small constant time, speed loop
Tetm=Tdt+Ttm;
%Imposed phase margin:
fimm=45*pi/180;
% a factor
a=(1+cos(fimm))/sin(fimm)

%%%%%%%%%%%%%%%%%%%%%%%%%%%%%%%%%%%%%%%%%%%%%%%%%%%%%%%%%%%%%%%%%%%%%%%%%%%%%%%%
%Tuning of the speed controller parameters kpt(1+sTit)/sTit %
%%%%%%%%%%%%%%%%%%%%%%%%%%%%%%%%%%%%%%%%%%%%%%%%%%%%%%%%%%%%%%%%%%%%%%%%%%%%%%%%

kpt=J/(a*Tetm); Tit=a^2*Tetm

%%%%%%%%%%%%%%%%%%%%%%%%%%%%%%%%%%%%%%%%%%%%%%%%%%%%%%%%%%%%%%%%%%%%%%%%%%%%%%%%
%Speed regulator of type1: kp_om+ki_om/s, Kessler %
%%%%%%%%%%%%%%%%%%%%%%%%%%%%%%%%%%%%%%%%%%%%%%%%%%%%%%%%%%%%%%%%%%%%%%%%%%%%%%%%

kp_om=kpt; ki_om=kpt/Tit

%%%%%%%%%%%%%%%%%%%%%%%%%%%%%%%%%%%%%%%%%%%%%%%%%%%%%%%%%%%%%%%%%%%%%%%%%%%%%%%%
% Speed regulator of type2: (1+s*tau3)/s*tau4 %
%%%%%%%%%%%%%%%%%%%%%%%%%%%%%%%%%%%%%%%%%%%%%%%%%%%%%%%%%%%%%%%%%%%%%%%%%%%%%%%%

tau3=4*Tetm; tau4=8*Tetm^2/J
%%%%%%%%%%%%%%%%%%%%%%%%%%%%%%%%%%%%%%%%%%%%%%%%%%%%%%%%%%%%%%%%%%%%%%%%%%%%%%%%
```

```
% Speed regulator of type3: kp_omk+ki_omk/s   %
%%%%%%%%%%%%%%%%%%%%%%%%%%%%%%%%%%%%%%%%%%%%%%%
kp_omk=tau3/tau4       %Kessler
ki_omk=1/tau4
%%%%%%%%%%%%%%%%%%%%%%%%%%%%%%%%%%%%%%%%%%%%%%%%%%%%%%%%%%%%%%%%%%%%%%%%%%%%
%Flux loop (d axis)_ approximated mathematical model 1/(s*Tr/Lm): Kessler %
%%%%%%%%%%%%%%%%%%%%%%%%%%%%%%%%%%%%%%%%%%%%%%%%%%%%%%%%%%%%%%%%%%%%%%%%%%%%
% Flux regulator of type1: (1+s*tau3f)/s*tau4f
Tr=Lr/Rr;%rotor time constant
tau3f=4*Tetm
tau4f=8*Tetm^2/(Tr/Lm)
% Flux regulator of type2: kp_dfk+ki_dfk/s
kp_dfk=tau3/tau4
ki_dfk=1/tau4
%%%%%%%%%%%%%%%%%%%%%%%%%%%%%%%%%%%%%%%%%%%%%%%%%%%%%%%%%%%%%%%%%%%%%%%%%%
% Flux loop (d axis) approximated mathematical model 1/(s*Tr/Lm): Blasko%
%%%%%%%%%%%%%%%%%%%%%%%%%%%%%%%%%%%%%%%%%%%%%%%%%%%%%%%%%%%%%%%%%%%%%%%%%%
% from closed loop d axis current transfer function
Tfm=2*Teim   %the same with  Ttm
%delay time constant of the flux loop sample and hold device
Tdf=Ts;
%time delay constant of the sample and hold device
Tefm=Tdt+Tfm;
%Reference of the phase margin:
fimf=60*pi/180;
% af factor
af=(1+cos(fimf))/sin(fimf)

%%%%%%%%%%%%%%%%%%%%%%%%%%%%%%%%%%%%%%%%%%%%%%%
% Speed regulator of type 3:kpf(1+sTif)/sTif  %
%%%%%%%%%%%%%%%%%%%%%%%%%%%%%%%%%%%%%%%%%%%%%%%
kpf=(Tr/Lm)/(a*Tefm)
Tif=a^2*Tefm
%%%%%%%%%%%%%%%%%%%%%%%%%%%%%%%%%%%%%%%%%%%%%%%%
% Flux regulator of type 3: kp_df+ki_df/s      %
%%%%%%%%%%%%%%%%%%%%%%%%%%%%%%%%%%%%%%%%%%%%%%%%
kp_df=kpf; ki_df=kpf/Tif
```

Acknowledgements

This work was supported by a grant of the Romanian National Authority for Scientific Research, CNDI– UEFISCDI, project number PN-II-PT-PCCA-2011-3.2-1680.

Author details

Marian Gaiceanu*

Dunarea de Jos University of Galati, Romania

http://dx.doi.org/10.5772/57521

References

[1] Athans M. & P. L. Falb (2006). Optimal Control: An Introduction to the Theory and Its Applications. ISBN: 0486453286, USA, Dover, 2006

[2] COM(2006). Action Plan for Energy Efficiency: Realising the Potential, Available from

[3] Gaiceanu, M. (1997). "Optimal Control for the Variable Speed Induction Motor"- thesis dissertation Master Degree, Power Electronics and Advanced Control Methods of the Electromechanical Systems, Dunarea de Jos University of Galati, June 1997

[4] Gaiceanu, M. (2002). Ph.D. thesis Optimal Control of the Adjustable Electrical Drive Systems with Induction Motors by using Advanced Methods, Dunarea de Jos University of Galati, April, 2002, Romania

[5] Gaiceanu, M., Rosu E., Paduraru R. & Dache C. (2008). Optimal Control Development System for Electrical Drives, *The Annals of "Dunarea de Jos" University of Galati*, FASCICLE III, Vol.31, No.1, ISSN 1221-454X, pp. 5-10.

[6] Gattami A. & Rantzer A. (2005). Linear Quadratic Performance Criteria for Cascade Control, Proceedings of the 44th IEEE Conference on Decision and Control, and the European Control Conference 2005 Seville, Spain, December 12-15, 2005

[7] http://ec.europa.eu/energy/action_plan_energy_efficiency/doc/com_2006_0545_en.pdf

[8] http://www.automation.siemens.com/

[9] Jianqiang, L., Yang, L., F., Zheng, Z., Trillion., Q. (2007). *Optimal Efficiency Control of Linear Induction Motor Drive for Linear Metro*, 2nd IEEE Conference on Industrial Applications, 2007, ICIEA 2007, 23-25 May 2007, pp. 1981-1985, ISBN 978-1-4244-0737-8, 2007

[10] Leonhard, W.: *Control of Electrical Drives*, Springer-Verlag, Berlin 1996

[11] Lorenz, R. D., Yang S.-M. (1992). "Efficiency-Optimized Flux Trajectories for Closed-Cycle Operation of Field-Orientation Induction Machines Drives", IEEE Trans. Ind. Appl.,Vol. 28, No. 3, May/Jun. 1992, pp. 574-580.

[12] Lorenz, R. D., Yang, S.M. (1998). "Efficiency-Optimized Flux Trajectories for Closed Cycle Operation of Field Oriented Induction Machine Drives", Industry Applications Society Annual Meeting, 1988., Conference Record of the 1988 IEEE, pp 457-462, 1998

[13] Matinfar, M., K.Hashtrudi-Zaad (2005). Optimization-based Robot Compliance Control: Geometric and Linear Quadratic Approaches, International Journal of Robotics Research, ISSN 0278-3649, Sage Publications, Inc., Vol.24, pp. 645-656, August 2005

[14] Mendes, E., A. Baba, A. Razek, (1995). "Losses Minimization of a Field Oriented Controlled Induction Machine", Proceed. of IEE Electrical Machines and Drives Conf., Sep. 1995, pp. 310-314.

[15] Rosu, E. (1985). A Solution of Optimal Problem with Quadratic Performance Criteria, Analele Universitatii "Dunarea de Jos" Galati

[16] Rosu, E., Gaiceanu, M., & Bivol, I. (1998). Optimal Control Strategy for AC Drives, PEMC '98, 8th International Power Electronics & Motion Control Conference, Prague, Czech Republic, pp.4.160-4.165

[17] Rosu, E., Gaiceanu, M., Bivol, I. (1998). "Load Torque Estimation for AC Motors", CNAE '98, The 9th Symposium on Electrical Drives, Craiova, Romania, ISBN 973-9346-68-5, pp. 221-224, 1998

[18] Su, C.T. & Chiang C.L. (2004). Optimal Position/Speed Control of Induction Motor Using Improved Genetic Algorithm and Fuzzy Phase Plane Controller, Journal of Control and Intelligent Systems, ISSN 1480-1752, Vol.32, 2004

[19] Tamimi, J.M.Kh. & Jaddu, H.M. (2006). Optimal vector control of three-phase induction machine, International Association of Science and Technology for Development, Proceedings of the 25th IASTED International Conference on Modeling, Identification and Control, Lanzarote, Spain, Acta Press, CA USA, ISSN 0-88986-549-3, 2006, pp. 92-96

[20] Veerachary M. (2002). Optimal control strategy for a current source inverter fed induction motor, Computers and Electrical Engineering, Vol.28, No.4, July 2002, pp. 255-267

[21] Vukosavic, S.N., Jones, M., Levi, E., and Varga J. (2005). Rotor flux oriented control of a symmetrical six-phase induction machine, Electric Power Systems Research 75 (2005) 142–152